AD-A063 824 GHANA UNIV LEGON DEPT OF PHYSICS F/G 4/1
PHASE AND AMPLITUDE SCINTILLATION AT THE EQUATOR.(U)
OCT 78 J R KOSTER AFOSR-78-3516
UNCLASSIFIED AFGL-TR-78-0298 NL

| OF |
AD A063 824

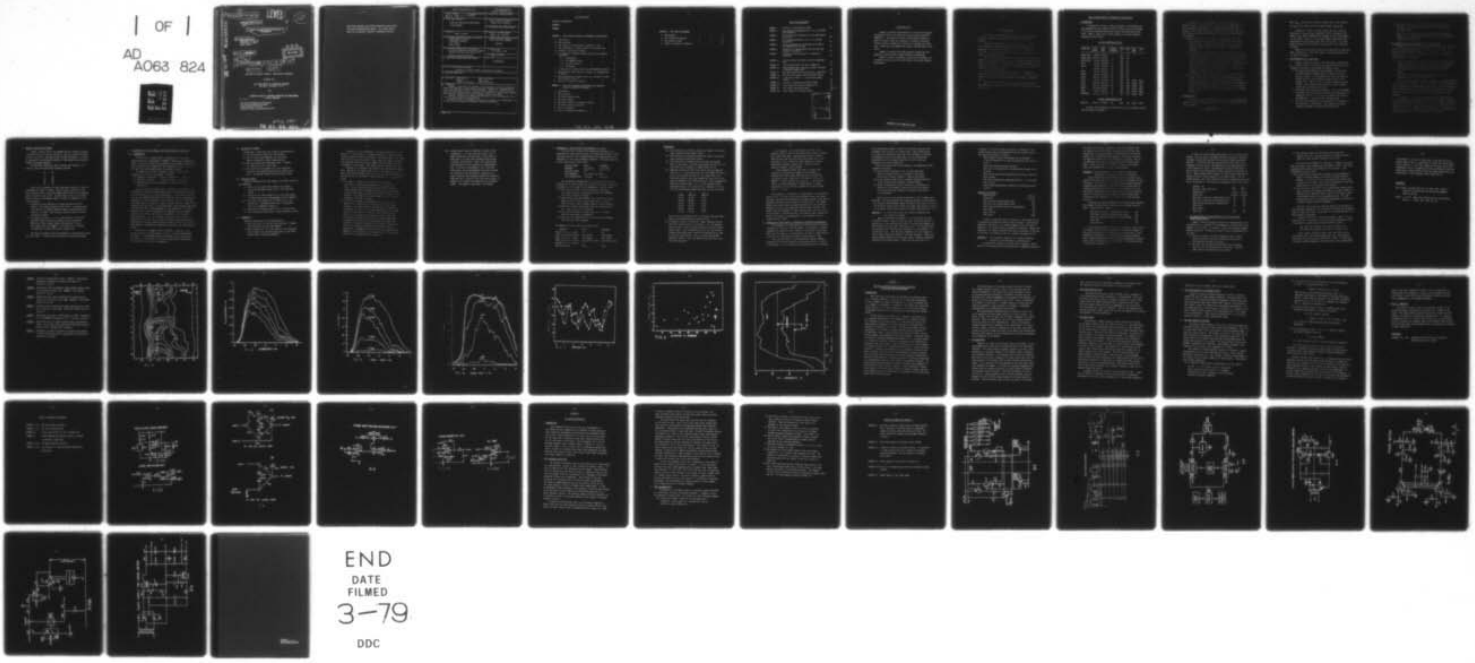

END
DATE FILMED
3-79
DDC

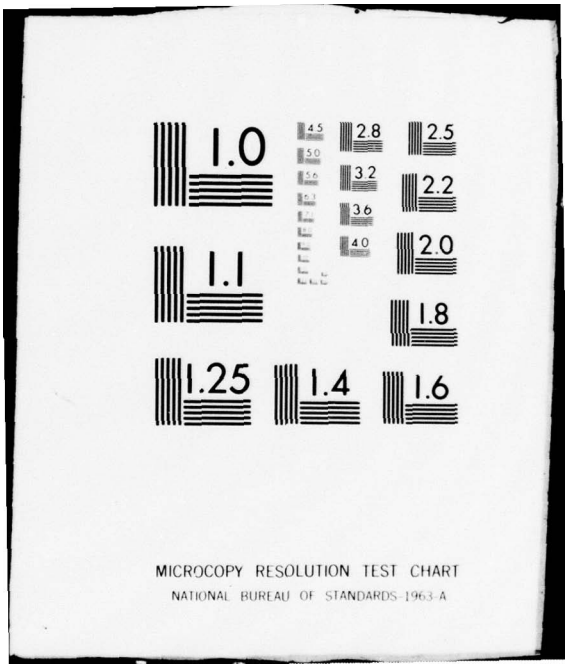
1.0
1.1
1.25
1.4
1.6
1.8
2.0
2.2
2.5
2.8
3.2
3.6
4.0
4.5
5.0
5.6
MICROCOPY RESOLUTION TEST CHART
NATIONAL BUREAU OF STANDARDS-1963-A

DDC FILE COPY AD A063824

(18) AFGL (19) TR-78-0298

LEVEL II

12

GRANT NO (15) AFOSR-78-3516

(6) PHASE AND AMPLITUDE SCINTILLATION AT THE EQUATOR.

(10) John R. Koster
Department of Physics
University of Ghana
Legon, Ghana.

DDC
RECEIVED
JAN 26 1979
C

(11) 31 Oct 78

(12) 55 p.

(9) Final Scientific Report. 1 Feb - 31 Oct 78.

(16) 4643 (17) 05

Approved for public release: distribution unlimited

Prepared for:

AIR FORCE OFFICE OF SCIENTIFIC RESEARCH
Arlington, Virginia, U.S.A.

and

EUROPEAN OFFICE OF AEROSPACE RESEARCH AND DEVELOPMENT
London, England.

62101F

Air Force Geophysics Laboratory
Air Force Systems Command
United States Air Force
Hanscom AFB, Massachusetts 01731

402 565

79 01 26 030

Qualified requestors may obtain additional copies from the Defense Documentation Center. All others should apply to the National Technical Information Service.

REPORT DOCUMENTATION PAGE	READ INSTRUCTIONS BEFORE COMPLETING FORM
1. Report Number AFGL-TR-78-0298 2. Govt Accession No.	3. Recipient's Catalog Number
4. Title (and Subtitle) PHASE AND AMPLITUDE SCINTILLATION AT THE EQUATOR	5. Type of Report & Period Covered Final Scintific Report 78 Feb. 01 - 78 Oct. 31
	6. Performing Org. Report Number
7. Author(s) JOHN R. KOSTER	8. Contract or Grant Number AFOSR - 78 - 3516
9. Performing Organization Name and Address Department of Physics University of Ghana P.O. Box 63 Legon, Ghana	10. Program Element, Project, Task Area & Work Unit Numbers 46430502
11. Controlling Office Name and Address Air Force Geophysics Laboratory (AFSC) Hanscom Air Force Base, Mass. 01731 Monitor/John Mullen/PHP	12. Report Date 31 October, 1978 13. Number of Pages 56
14. Monitoring Agency Name and Address	15. UNCLASSIFIED
16. & 17. Distribution Statement Approved for public release; distribution unlimited.	
18. Supplementary Notes	
19. Key Words Scintillation Equator Annual distribution Depth of Fading Onset time Time distribution	

20. Abstract.

Chapter 1 describes some features of new and more accurate scintillation data at 257 MHz from a high elevation satellite (MARISAT 1). Observations at Legon yield improved results on depth of fading, fading as a function of elevation, and some initial results on fading as a function of frequency and longitude. These data are compared with earlier 136 MHz results from Legon.

Chapter 2 describes the phase switching system used for making the above satellite signal amplitude measurements.

Chapter 3 gives a description, with circuit diagrams, of a polarimeter used at Legon for both digital and analogue Faraday measurements.

FORM 1473

CONTENTS

79 01 26 030

CHAPTER 3. THE LEGON POLARIMETER.

LIST OF ILLUSTRATIONS

ACCESSION for
NTIS [illegible] Section
DDC Buff Section
UNANNOUNCED
JUSTIFICATION
BY
DISTRIBUTION/AVAILABILITY CODES
Dist SPECIAL

ABSTRACT

Chapter 1 describes some features of new and more accurate scintillation data at 257 MHz from a high elevation satellite (MARISAT 1). Observations at Legon yield improved results on depth of fading, fading as a function of elevation, and some initial results on fading as a function of frequency and longitude. These data are compared with earlier 136 MHz results from Legon.

Chapter 2 describes the phase switching system used for making the above satellite signal amplitude measurements.

Chapter 3 gives a description, with circuit diagrams, of a polarimeter used at Legon for both digital and analogue Faraday measurements.

PRECEDING PAGE BLANK-NOT FILMED

FOREWORD

This report covers experimental work done over the period 1-10-77 to 30-6-78. Earlier data are included in many of the analyses.

Gratitude is expressed to Mr. S.K. Osei, Mr. H. Anum and Mr. T. Decker for the routine operation and maintenance of the equipment. Thanks are also expressed to Mr. Philip Kwaku and Mr. E. Egah for data reduction and key punching and to Mr. T.K. Quartey for typing the report.

Further Faraday rotation results from Legon using a satellite (SIRIO) at a relatively high elevation are currently being obtained. These 136 MHz results can eventually be compared with earlier results at the same frequency; at the moment the data base is too small to render such a study practicable.

The chapter (2) on scintillation measuring equipment is included, since the scintillation results at low elevations and low signal strengths are highly dependendant on the type of equipment used.

The chapter on the polarimeter is included for the record. Much Faraday data appears in previous reports - this is the equipment used to get it.

SOME FURTHER STUDIES OF EQUATORIAL SCINTILLATION

1. INTRODUCTION

A considerable volume of data on equatorial scintillation has been obtained at Legon, Ghana (5.63°N, -0.19°E), since the launching of the first synchronous satellites visible from that part of the world. Table 1 below gives a brief summary of the data presently available at the station.

136 MHz SCINTILLATION DATA

SATELLITE	DATE BEGINS	DATE ENDS	SPACING IN MINUTES	CARDS ?	DISK ?	FILE NAME	DISK
Early Bird	23-5-65	12-8-65	5	YES	NO		
Canary Bird	18-5-67	23-5-68	5	YES	NO		
Early Bird	9-4-69	26-6-69	5	YES	NO		
ATS-3	2-7-69	22-12-69	5	YES	NO		
ATS-3	4-6-70	1-4-71	10	YES	NO		
"	4-6-70	30-6-70	15	YES	NO		
IS2F2	5-4-71	17-5-71	10	YES	NO		
IS2F2	9-6-71	29-8-71	10	YES	NO		
ATS-3	30-8-71	5-10-71	10	YES	NO		
ATS-3	1-9-71	27-11-76	15	YES	YES	S1136	Ø3AD
IS2F2	6-10-71	28-9-72	15	YES	YES	SI2ND	1AFC
IS2F3	28-9-72	16-11-74	15	YES	YES	SI2ND	1AFC
GOES 1	27-11-76	27-4-77	15	YES	YES	S1136	Ø3AD
ATS-5	5-5-77	30-6-78	15	YES	YES	S1136	Ø3AD
SYMPHONIE	1-11-76	31-1-77	15	YES	YES	SYM76	Ø3AD

257 MHz SCINTILLATION DATA

Marisat 1	16-3-77	30-6-78	15	YES	YES	S1257	1AFC

The most recent addition to this data is that on 257 MHz, recorded from the satellite MARISAT 1.

The recording of the amplitude of the 257 MHz signal from Marisat 1 began on 16 March, 1977. The usual phase switch was used in a total power configuration. A 30 foot paraboloid was used as antenna. This yielded a signal at least 20 db above the noise level. As a result of this excellent signal to noise ratio, three possibilities emerged:

(1) With this system it is possible to measure very deep fades with reasonable accuracy. With most other satellite signals used at Legon, the signal is much closer to the noise level, and fades deeper than about 10 db cannot be measured with accuracy.

(2) As a result of the strong signal, a short time constant could be used in the output of the phase sensitive detector, and still maintain a good signal to noise ratio. This results in accuracy in the measurements of relatively fast fades. In practice, a time constant of 0.22 seconds was used in the output of the phase sensitive detector. The limiting factor was the Easterline-Angus chart recorder used in the experiment. It has a time constant of between 1 and 2 seconds.

(3) "Saturation" effects occur frequently in equatorial fading records. These are more severe for lower frequencies, and for lower elevation sources. The combination of high elevation (71°) and relatively high frequency (257 MHz) in this experiment reduced these saturation effects and gave a much more accurate picture of the effects of equatorial scintillation on a communication signal.

2. DATA ANALYSIS

The analysis of the fading records was done as previously determining the scintillation index (S.I.) for each 15 minute interval from the expression:

$$S.I. = \frac{P_{mx} - P_{min}}{P_{max} + P_{min}} \times 100$$

where P_{max} is the power of the 3rd highest peak in the interval, and P_{min} is the power of the 3rd lowest trough respectively.

In addition to this, a second anlysis was made, using the difference of P_{max} and P_{min} expressed in db as a measure of the fading. This latter method is more suitable for the investigation of deep fading, since the scintillation index crowds most of the deep fades into the extreme upper limit of the scale. All fades deeper than 16 db, for instance, are crowded into the last 5% of the scale.

These data were stored on disk files identified as SI257 and DB257, respectively. Both files cover the interval from 16-3-77 to 30-6-78, inclusive.

3. THE CONTOURS OF S.I. FOR A YEAR

Figure 1 shows the contours of the percentage occurrence of SI > 60 for a period of just over one year, (16-3-77 to 30-3-78). A number of features in the diagram are worthy of note:

a. The equinoctial maxima are very prominent. The fact that the March maximum is higher than the October one is not typical, however. It is probably due to the fact that the period covered is on the rapidly rising portion of the sunspot cycle. March '78 saw a dramatic increase in solar activity, with corresponding increases in total electron content and scintillation activity.

b. The maxima occur well before midnight. This is in agreement with past Legon results where saturation effects were not a significant factor. It is also in agreement with results from Huancayo (J. Mullen, private communication).

c. The very steep evening rise in scintillation, especially at the equinoxes, is noteworthy. This indicates an almost explosive beginning of equatorial scintillation.

d. The onset of scintillation follows ground sunset by one or two hours. But the contours do not follow the local sunset line very closely.

e. There is little scintillation around the sunrise hours before November, '77. After that, it is present, but the scintillation indices are relatively low.

4. THE PROBABILITY OF VARIOUS LEVELS OF S.I. AGAINST TIME

Figure 2 shows a plot of the probability of occurrence of various levels of scintillation index as a function of time of night. These curves are derived from an analysis of all the data taken during the period 16-3-77 to 31-3-78. Attention is called to the following characteristics of the curves:

a. The post-sunset rise is almost simultaneous for all scintillation levels. This reflects the fact that the onset of scintillation is abrupt and is normally characterized by very deep fading.

b. The deepest fades reach their peaks first, and fall off soonest.

c. The lower levels of fading peak progressively later, and disappear later than the more intense ones.

The above characteristics suggest a maximum in irregularity production shortly after ionospheric sunset. Later scintillation is possibly due to somewhat older irregularities, from which the smallest scale sizes have already disappeared. The progressive disappearance of the lower levels of scintillation activity as the night progresses is to be expected.

In addition to the above, two smaller samples, centred on the October and March equinox respectively, were investigated. The curves agree in most respects with Figure 2. One small difference is that all curves rise initially to nearly the same height. The fall-off is similar to the above. This is not surprising, since the higher scintillation levels tend to be most frequent at the equinoxes.

5. MARISAT 1 AND DEPTH OF FADING

Figure 3 shows a plot of the probability that fading on Marisat 1 exceeds levels of 0,5,10,15, and 20 db. The plot covers the period 16-3-77 to 31-3-78 — the same as that covered in Figure 2. It gives an indication of scintillation depth at a time midway between sunspot minimum and sunspot maximum.

To facilitate comparison with SI curves shown earlier, it is useful to note the relationship between SI and DB

DB	SI
0	00
5	52
10	82
15	94
20	98

These curves represent the best Legon data available to date for determining the depth of fading. They are useful inasmuch as they show the distribution of very deep fades better than the corresponding plots of various levels of SI. We would like to point out, however, that the curve for the deepest fades (> 20 db) is probably too low, for two reasons.

a. Calibrations were initially not always extended carefully enough to the region around the noise level. An extrapolation then used by the computer program tended to underestimate the depth of the fades. This fault was corrected near the end of the period covered.

b. The relatively long (1 - 2 sec.) time constant of the chart recorder reduced the depth of fading at high frequencies. This would tend to reduce fading depths around 21 hours, when fading rates are highest. It is difficult to estimate the magnitude of this effect at the present time.

For these two reasons, the 20 db probability curve should be taken as a lower limit. A more accurate curve may be considerably higher.

6. A COMPARISON OF MARISAT RESULTS WITH RESULTS OBTAINED FROM ATS-5

6.1. INTRODUCTION

At this stage it seems useful to compare some of the curves obtained from the observations of MARISAT 1 with curves obtained from ATS-5. The latter satellite was observed on a frequency of 136.47 MHz, and it was located at roughly 70° west longitude, so that it was about 11° above the western horizon for an observer in Legon.

In comparing the curves, we must be aware of at least three factors that can affect our results. They are:

(a) Differing frequencies - 136.47 and 257.54 MHz respectively.
(b) Differing elevation - 11° and 70° respectively, and
(c) Differing receiver time constants - 0.22 sec and 4.0 sec respectively.

We might mention in passing that, surprising as it may seem, the difference in frequency between the two sets of observations is probably the least important of the three differences. This remark is based on the fact that MARISAT and SIRIO (136.14 MHz) were being recorded simultaneously on adjacent channels of a strip chart recorder. These two satellites were at virtually the same elevation, and their receiver time constants were identical. A rough comparison of the records showed that they were virtually indistinguishable to the unaided eye. A careful analysis with accurate calibrations will probably show an enhanced scintillation index at low levels of scintillation for the lower frequency signal - but the difference will surely not be great. It seems fair to say that, of the three differences being considered, the difference in frequency probably has the smallest effect on our curves. Much greater differences are introduced by elevation and time-constant effects.

We here wish to compare curves for MARISAT 1 and ATS-5. The curves for ATS-5 cover the period 1-11-77 to 31-3-78, and are shown in Figure 4. Corresponding curves for MARISAT over the same period were drawn, but since they do not differ significantly from Figure 2, the latter will be used in the comparison.

6.2. THE MARISAT 1 CURVES

The Marisat 1 curves have the following characteristics:

i. The scintillation curves rise very sharply.

ii. All the levels rise together; the curves are almost coincident in their rising portions.

iii. The peak values occur relatively early - between 21 hours and 22 hours local time.

iv. The curves are well spread out on the descending portions, scintillation becoming less probable with time. The severer scintillation disappears first.

6.3. THE ATS-5 CURVES

The main characteristics that appear in the ATS-5 curves are the following:

i. Curves for the lower level indices rise sharply; those for the higher levels of S.I. rise much more slowly.

ii. Curves for the lower values of S.I. rise much higher for ATS-5 than do the corresponding ones for MARISAT 1.

iii. The tops of the curves for low values of S.I. are almost flat - indicating some sort of "saturation" that is not apparent in Figure 2.

iv. The curves for higher values of S.I. are much lower.

v. Their peaks occur much later - around midnight or later.

6.4. DISCUSSION

Two main features are to be discussed here.

a. Lower levels of S.I. are much more frequent on signals from ATS-5 than on those from MARISAT.

b. Higher levels of S.I., on the contrary, are relatively less frequent, and rise much more slowly on the ATS-5 signals than on those from MARISAT.

Feature (a) is not surprising. One would expect more scintillation on a signal from a low elevation satellite , since it passes through a greater effective thickness of ionosphere than does a signal that comes from near the zenith. Hence, one would expect the curve for SI greater than 0% to be both higher, and also wider, than its counterpart from overhead. This agrees with the experimental curves.

Feature (b) is somewhat less obvious, and requires some explanation. Why should the higher levels of S.I. rise more slowly, peak later, and reach relatively lower levels for the low elevation satellite than for the one at the zenith? Three possible factors suggest themselves:

i. It could be a matter of the difference of frequency. But further investigation showed that this is not the case. Curves from the Italian satellite SIRIO, recorded using equipment nearly identical with that used for MARISAT yielded curves almost identical with those for MARISAT. The curves are not shown here, since the data reduction was not finished at the time of writing.

ii. It could be a matter of instrumentation - specifically, a matter of the different time constants used in the output circuit of the phase sensitive detector used. In the case of MARISAT, this was 0.22 seconds (made possible by the high signal to noise ratio). But in the case of ATS-5, and of most of the scintillation measurements made at Legon with relatively weak signals (due both to low aerial gains and low radiation levels from the satellites) the output time constant was typically between 4 and 6 seconds. This would lead to the selective attenuation of the higher fading frequencies. Measurements made on ATS-3 (low elevation) and Symphonie (high elevation) are discussed below. Both sets of curves show the characteristics of Figure 4.

iii. A third factor that can contribute is what we call "saturation". At lower elevation levels, and at lower frequencies, the mean level of the signal is often seen to be very much attenuated during times of severe scintillation. Hence, the scintillation index derived from such signals is correspondingly low. It would be interesting to use a very high aerial gain, and correspondingly short time constant on a satellite near the horizon, especially at a lower frequency, and determine whether the diminution comes mainly as a result of the long time constant, or whether it is largely contributed by the ionosphere itself. The answer is not clear at the moment.

7. COMPARISON OF CURVES DERIVED FROM SYMPHONIE AND GOES 1

To throw further light on the discussion appearing above, a comparison was made between results of simultaneous records obtained from two satellites which radiated signals at essentially the same frequency, but with very different elevations. The main facts about the two satellites are given below:

SATELLITE NAME:	GOES 1	SYMPHONIE
FREQUENCY:	136.380 MHz	137.200 MHz
ELEVATION ANGLE:	06°	71°
DATES OBSERVED	1-11-76/31-1-78	Same
TIME CONSTANT USED:	6 seconds	4 seconds

The probability distribution of S.I. was plotted for each satellite at the usual levels (>0, > 20, > 40, > 60, > 80). The following points are to be noted in the comparison of the two curves:

(a) The curves for GOES 1 (the low elevation satellite) rose higher than the corresponding curves for SYMPHONIE (the high elevation satellite).

(b) Both showed a much more gradual rise, especially for S.I. greater than 40, than do the curves shown in Figure 2. They much more closely resemble Figure 4 in this respect.

(c) Both show a broad, flat-topped curve for lower levels of S.I., much as do those of Figure 4.

(d) The curves for GOES 1 are also wider (i.e. of longer duration) than those for SYMPHONIE.

(e) The curves for higher levels of S.I. for both satellites had peaks well after midnight.

We summarize the main facts in the table below:

SATELLITE	GOES 1	SYMPHONIE
Height of S.I. > 0 curve	76	48
Width at half-power points	540 minutes	435 minutes
Shape of low S.I. curves	Flat topped	Flat topped
Shape of high S.I. curves	Peak after 0 Hours	Peak after 0 Hours
Height of S.I. > 80 curve	20	14
GMT of mid-point	00:30	00:00

CONCLUSIONS

(a) The difference in elevation affects the height of the curves. Lower elevations yield higher curves.

(b) The difference in elevation affects the width of the curves. Lower elevations yield wider curves.

(c) The difference in elevation does not affect the general shape of the curves. Both are flat-topped for low S.I., and have peaks after midnight for higher values of S.I.

(d) Midpoints between the half power points show the expected time lag, i.e., the western satellite lags behind the eastern one in time by about 30 minutes. The amount that a low elevation satellite curve lags behind the curve for an overhead one depends on the effective height of the irregularities causing the scintillation, i.e., on the location of the ionospheric point. For satellites at elevations of 6° and 71°, the corresponding heights and time lags are as follows:

	6°	71°
HEIGHT	TIME LAG	TIME LAG
100 km	23 min	1 min.
200 km	38 min.	2 min.
300 km	49 min.	4 min.
400 km	59 min.	5 min.
500 km	67 min.	6 min.
600 km	75 min.	7 min.

We note that our observed value of 30 minute time lag correspond to an effective height of about 200 km.

(e) A saturation effect is occurring. While elevation and the long time constant may both contribute to it, the evidence seems to point to the long time constant as the main contributing factor. This is supported by the fact that results obtained from SIRIO using a short time constant do not seem to show the same effects. This is a rather qualitative statement, however, since the SIRIO results have not as yet been fully analyzed.

The existence of this saturation effect has a very profound effect on most of the scintillation results obtained in the past from Legon. Whenever the satellite radiated power was low, and the aerial gain also rather low, it was necessary to use a rather long time constant to obtain a satisfactory signal to noise ratio. Values used were typically between 2 and 6 seconds.

This saturation effect can lead to a gross under-estimation of the depth of fading to be expected on communication links, where fading at higher frequencies is likely to play a major role. For such estimates, our MARISAT 1 results are much to be preferred. Even they may lead to an under-estimation of fading depths at higher frequencies, due to the time constant of the pen recorder used (1 - 2 sec.).

The appearance of saturation in Legon results is not something recent or new. The very first results obtained using radio stars and phase switching interferometers were characterized by the expected amplitude variations for low levels of scintillation. But deeper fading, especially around the equinoxes resulted in the total disappearance of radio star signatures from the chart records. The middle latitude standards of scintillation levels could not be used in the analysis of equatorial radio star results, and a simple scale based on the degree of disappearance of the signature had to be devised (Koster, 1958).

8. SCINTILLATION ONSET TIME AS A FUNCTION OF LONGITUDE AND ELEVATION

The dependence of scintillation on elevation and on longitude at Legon has never been fully determined. The problem is a rather difficult one unless one has a variety of satellites to work with. There have been quite a few satellites to the west of Legon over the years, but not very much to the east for any length of time.

Some start was made to the task when Mr. Lawrence Amaeshi analyzed scintillation results for three satellites over a period of six months. One of the rather puzzling things that he found was

that scintillation seemed to start on the western satellite more frequently than it did on one further east. Since scintillation is a night time phenomenon, and seems to be triggered in some way by ionospheric sunset, one might expect to find scintillation starting first on the eastern satellite of an E-W pair more frequently than on the western one.

The above results were rather puzzling, and immediately raised a number of questions:

(a) Is this result obtained if one uses much more data? Could it possibly just be a statistical fluctuation from using too small a number of cases in the study?

(b) Is the unusual result due to a genuine longitude variation in the frequency and intensity of scintillation?

(c) Could one explain the result in terms of a difference in elevation, since Amaeshi's eastern satellite was usually at a relatively high elevation; his western satellite at a low elevation?

Below we set out the investigation made to try to answer these questions. The data available for analysis consisted in the following:

(a) 15 minute scintillation Indices for ATS-3, from 1-9-71 to 21-10-76

(b) 15 minute scintillation Indices for IS2F2, from 6-10-71 to 28-9-72

(c) 15 minute scintillation Indices for IS2F3, from 28-9-72 to 16-11-74

QUESTION 1: Do other data on hand give results consistent with those found by Amaeshi?

Amaeshi considered his records on a "yes-no" basis for each 15 minute interval. Hence, we did the same. No use was made of the actual value of the scintillation index. In this first attempt, all the available data were used, 1138 days in all. The satellite ATS-3 was stationary at 70 degrees west longitude, at an elevation of 12° as seen from Legon. The satellite compared with it was always the east of ATS-3, though not always at the same longitude. IS2F2 moved slowly eastward during the period given above, eventually disappearing below the eastern horizon. IS2F3 rose from the west to an

elevation of about 80° during the period of observation, then slowly dropped again and disappeared below the western horizon. The data were treated as follows:

Data between 18 hours and midnight were considered.

A day was accepted if at least one satellite had a value of SI >0.

Days with missing data were rejected.

Days with no scintillation on either satellite were listed as quiet.

Days with scintillation appearing first on the E satellite were counted.

Days with scintillation appearing first on the W satellite were counted.

Days showing simultaneous inception of scintillation were counted.

RESULTS OF ANALYSIS 1

Beginning day:	6-10-71
Ending day:	16-11-74
Days with East scintillating first: . .	414
Days with West scintillating first: . .	461
Days with simultaneous onset of scintillation	146
Quiet days:	61
Days rejected:	56
Total days:	1138

It must be concluded that the results of a three year period of observation confirm the result found by Amaeshi. Scintillation began more frequently on the western member than on the eastern member of a two satellite pair, separated in longitude. During this experiment, the eastern satellite was above an elevation of 60° most of the time; the western one was at a constant elevation of 12°.

QUESTION 2: Is the unusual result due to a genuine longitude variation in the frequency of scintillation?

To answer this question, one would like to compare a large amount of simultaneous data from satellites at comparable elevations,

but with very different longitudes. This is not possible with our available data, since there is relatively little data from satellites to the east of Legon. IS2F2 did move to the eastern horizon, but it was moving very rapidly at that time, and only a few days were required for it to disappear completely. Most of the IS2F2 data are from much higher elevations than that from ATS-3. Hence, we leave this question, and move to the third, where our available data can give us some answers.

QUESTION 3: Can one explain the observations in terms of a difference in elevation of the two satellites?

This question was initially approached by including in the analysis only those nights on which scintillation appeared on both satellites. It has been observed that a low elevation satellite frequently shows relatively small scintillation indices when an overhead satellite shows none at all. This could be due to the much longer ionospheric path of the signal from the low elevation source; it could also be due to rather enhanced scintillation effects from rays incident on the ionosphere at near glancing incidence.

Initially, all other conditions in the anlysis were unchanged. Days showing scintillation on one satellite only were listed as quiet. Results were as follows:

Days with E satellite scintillating first:	391
Days with W satellite scintillating first:	318
Days with simultaneous start of scintillation:	167
Quiet days	202
Days rejected	60

The result now coincides with our expectation. On the average, the eastern satellite began to scintillate before the western one. The previous results seem to have been due to the effect of days having no scintillation at all on the high-elevation satellite. Both a longitude dependence and an elevation dependence of scintillation could contribute to the above result. The elevation seems to be the more important one.

A third and fourth analysis were made to try to clarify things further. For the third, only IS2F2 and ATS-3 were used. Data were confined to those days on which the elevation of IS2F2 was greater than 60°. This means that the satellite was within $\pm 25^{\circ}$ of the longitude of Legon, and the ionospheric point was within about $\pm 2^{\circ}$ of the longitude of Legon. The longitude of ATS-3 was 70° west of that of Legon, and the ionospheric point longitude for ATS-3 was at 12° W. Days considered were confined to those on which scintillation indices of 60% or greater appeared on the IS2F2 record. For the fourth analysis, data from IS2F3 and ATS-3 were considered in the same way as in analysis 3. The results are summarized in the table below:

ANALYSIS NO.	3	4
Satellite used: ATS-3 used	IS2F2	IS2F3
Starting date	7-10-71	27-1-73
Ending date	14-05-72	15-3-74
Days with E satellite scintillating first	90	121
Days with W satellite scintillating first	47	96
Days showing simultaneous scintillation	46	38
Quiet days	34	151
Days rejected	5	7
Total days	222	413

9. THE DISTRIBUTION OF SCINTILLATION AS A FUNCTION OF TIME USING EARLIER RESULTS

Figure 5 shows the percent occurrence of scintillation on the satellites Goes 1 (elevation 6°) and Symphonie (elevation 70°), from November '76 to January '77 inclusive. These data represent sunspot minimum conditions. Attention is called to three characteristics of the figure.

(1) The high elevation satellite (Symphonie) shows a lower percent occurrence than the low elevation one (Goes 1). This persists throughout the night.

(2) The curve for the high elevation satellite is narrower than that for the satellite near the horizon. The half-power points are sketched into the figure.

(3) The midpoint between the half-power points shows the expected time lag. The high elevation (eastern) satellite leads the lower elevation (western) one in time.

The curve shown in Figure 5 is typical of a family of 12 curves that were drawn - each representing three months of data. The characteristics mentioned above were present in all of them. A few differences are worth noting:

(1) As scintillation becomes more probable near the equinoxes, or nearer to sunspot maximum, the percent occurrence tends to saturate. In these cases the curves become more nearly equal in height and in width. But the time displacement of the point midway between the half-power points remains.

(2) If one plots the mean value of the scintillation index against time, instead of the percent occurrence, the curves exhibit the characteristics described above. But they also tend to show a more prominent peak in the pre-midnight period. This same characteristic has been mentioned in describing our results for a higher frequency satellite (MARISAT 1).

The above curves show why, when one observes two satellites at very different elevations, the low elevation satellite may frequently begin to scintillate first, even though it is positioned west of the high elevation counterpart.

A further remark can be made about analyses 3 and 4. If one takes the ratio of days with the east satellite scintillating first to days when the western one scintillates first, we get:

For IS2F2 (3rd analysis) the ratio is 90/47 or 1.91
For IS2F3 (4th analysis) the ratio is 121/96 or 1.26.

On the average, IS2F2 was further east than IS2F3, and we would expect that, other things being equal, that scintillation would more frequently begin on IS2F2 than on IS2F3. If there were a serious longitude dependence of scintillation, with scintillation

less probable to the east of Legon than to the west (as Basu's results seem to show), it would tend to reduce this ratio, rather than to enhance it. But other things are not equal in the above comparisons, and it is dangerous to draw any conclusion from them except that a large elevation effect can easily explain the above observations; a large longitude effect cannot do so.

REFERENCES

Basu, Sunanda, Santimay Basu and B.K. Khan, 1976 Model of equatorial scintillation from in-situ measurements Radio Sci.11,821.

Koster, J.R. 1955 Radio star scintillation at an equatorial station. J. Atmos. Terr. Phys. 12, 100.

FIGURE 1 Contours of Scintillation Index. MARISAT 1 (257.55 MHz) Percentage Occurrence of Scintillation Index > 60 16-3-77 to 31-3-78.

FIGURE 2 Probability that Scintillation Index exceeds various levels as a function of local time. MARISAT 1 (257.55 MHz) 16-3-77 to 31-3-78.

FIGURE 3 Probability that depth of fading in db exceeds various levels as a function of local time. MARISAT 1 (257.55 MHz) 16-3-77 to 31-3-78.

FIGURE 4 Probability that Scintillation Index exceeds various levels as a function of local time. ATS-5 (136.47 MHz) 1-11-77 to 31-03-78.

FIGURE 5 Percentage Occurrence of Scintillation on GOES 1 (Elevation = 6°) and SYMPHONIE (Elevation = 71°) 1-11-76 to 31-01-77..

FIGURE 6 Mean Daily Sum of 15 minute periods showing Scintillation Index > 10 for ATS-3 (Solid Dots) and IS2F2/IS2F3 (Circles) October 1972 to November 1974 inclusive.

FIGURE 7 Difference in number of periods of Scintillation records of ATS-3 and Intelsat-2F2 or Intelsat-2F3 as a function of elevation of Intelsat.

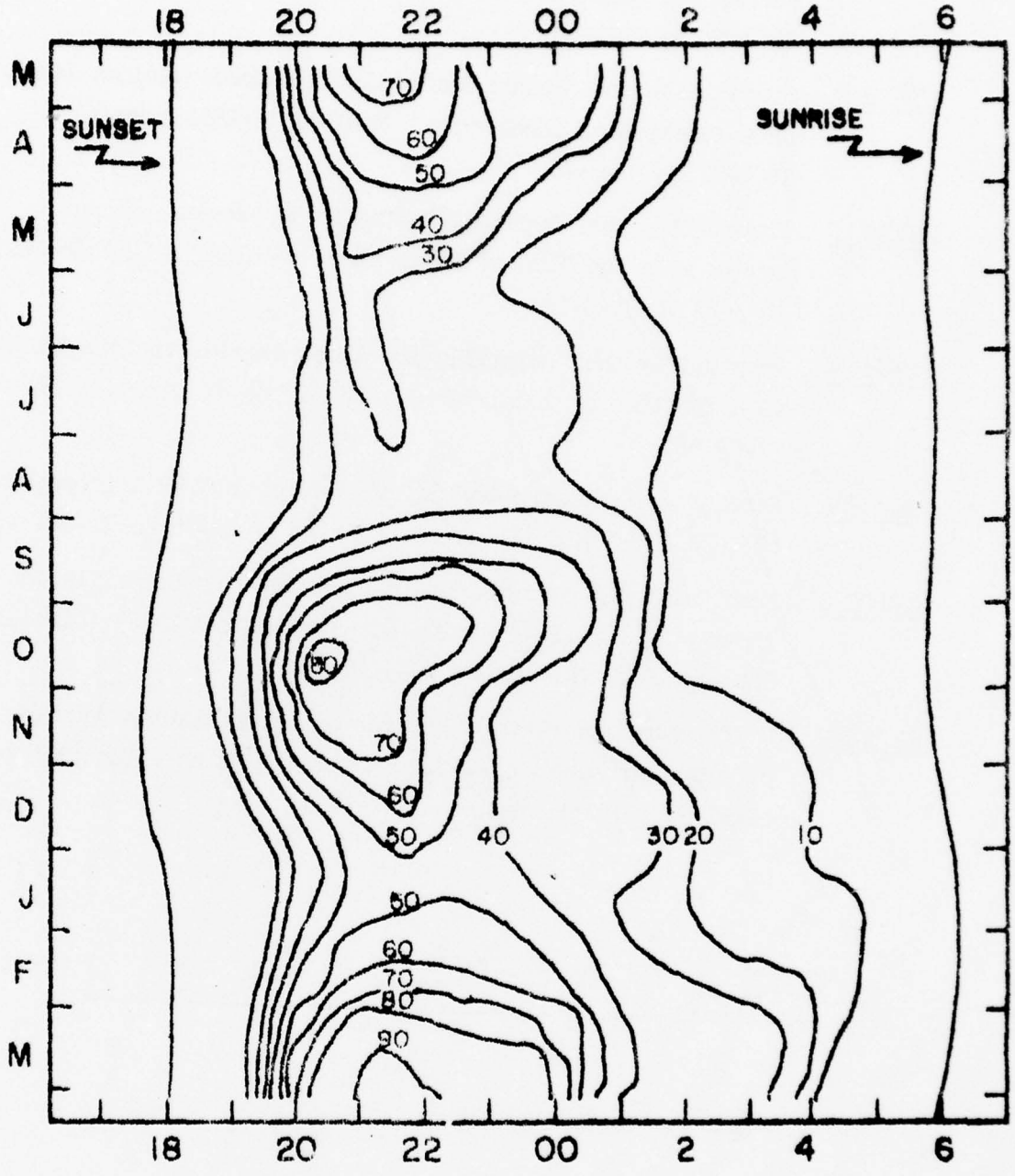
18
20
22
00
2
4
6
M
A
M
J
J
A
S
O
N
D
J
F
M
SUNSET
SUNRISE
70
60
50
40
30
80
70
60
50
40
30
20
10
50
60
70
80
90

Fig. 1

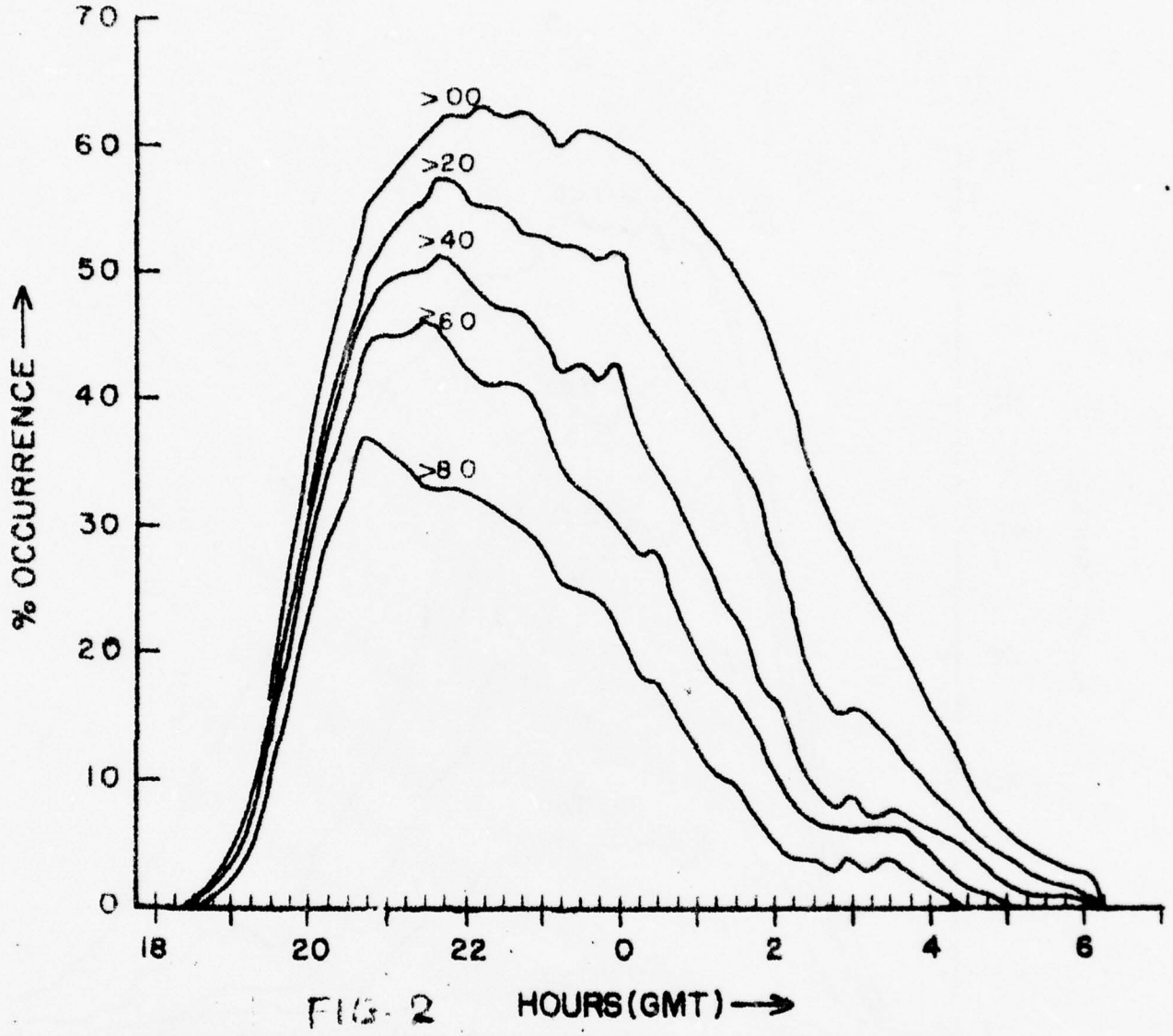
70
60
50
40
30
20
10
0
% OCCURRENCE →
>00
>20
>40
>60
>80
18
20
22
0
2
4
6
HOURS (GMT) →

FIG. 2

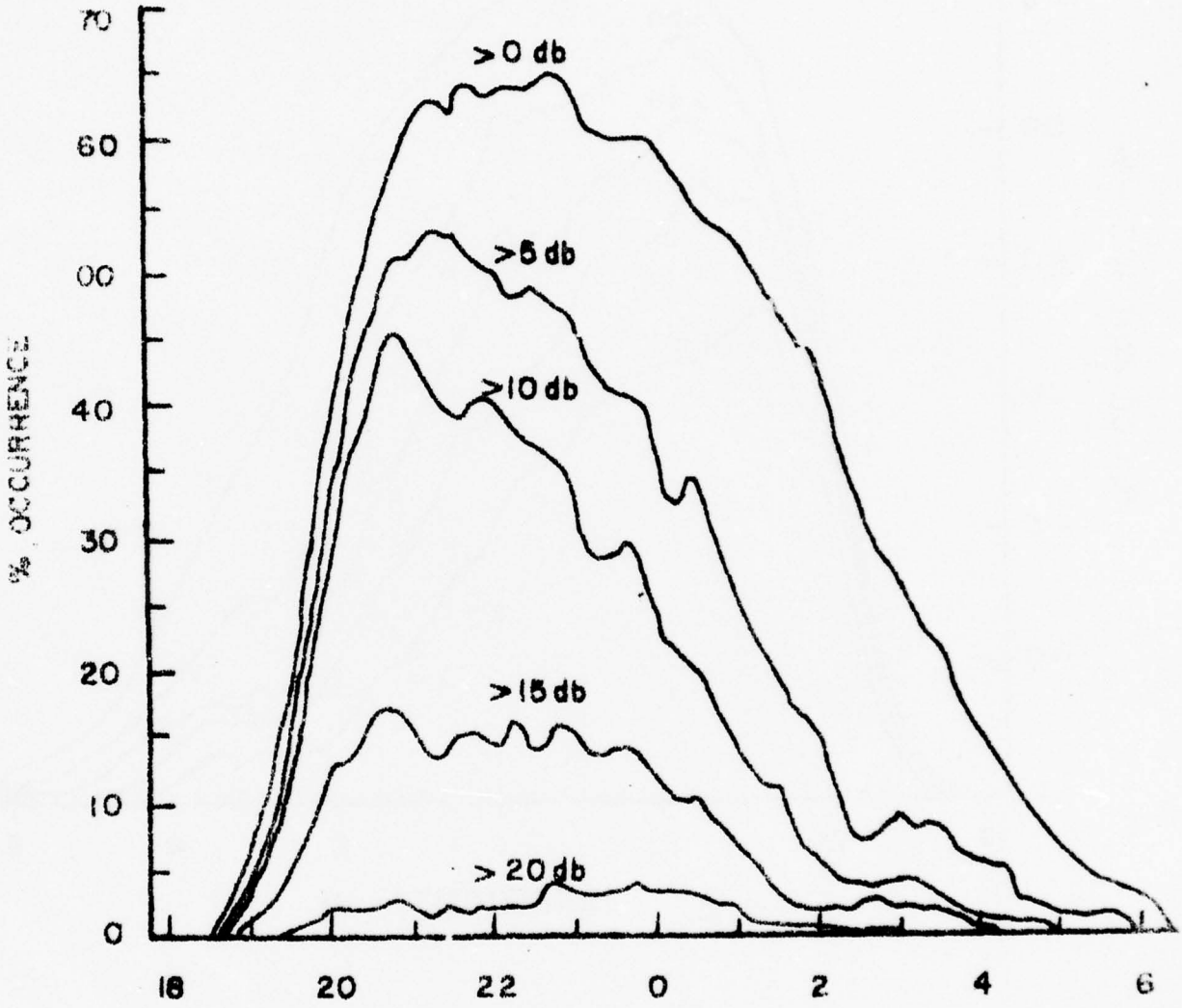
70
60
00
40
30
20
10
0
% OCCURRENCE
>0 db
>5 db
>10 db
>15 db
>20 db
18
20
22
0
2
4
6
HOURS (GMT) ⟶

FIG. 3

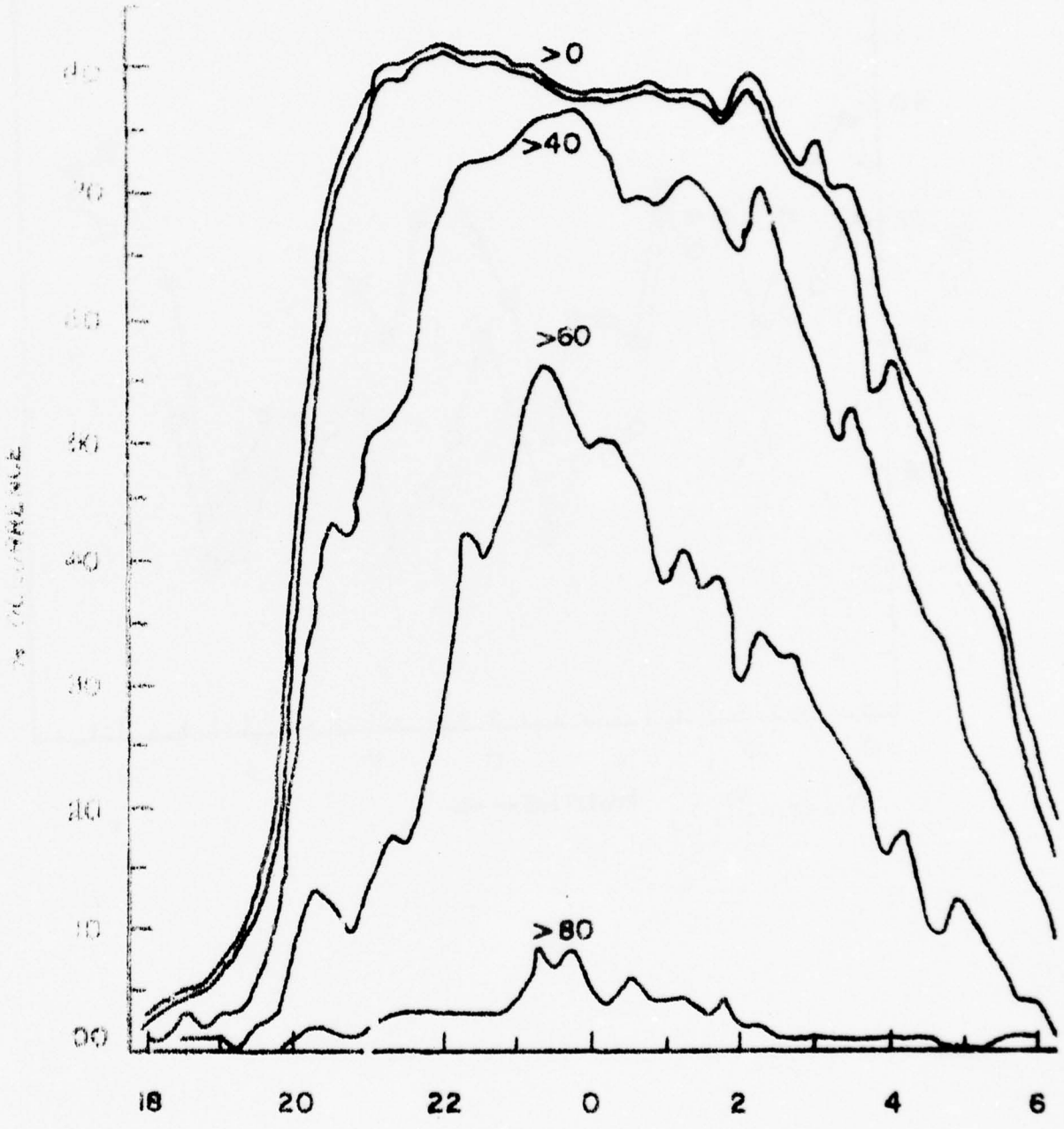

FIG. 4

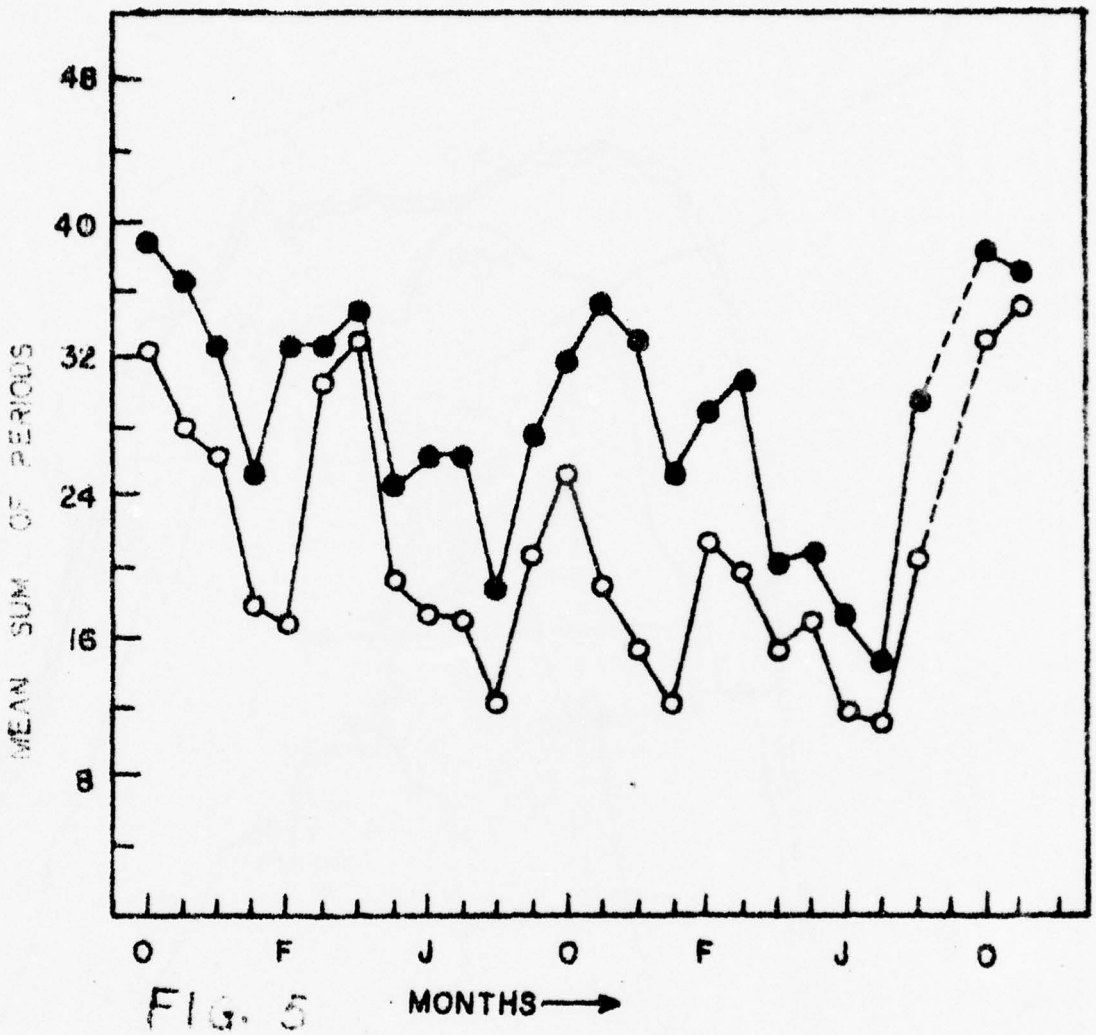

FIG. 5

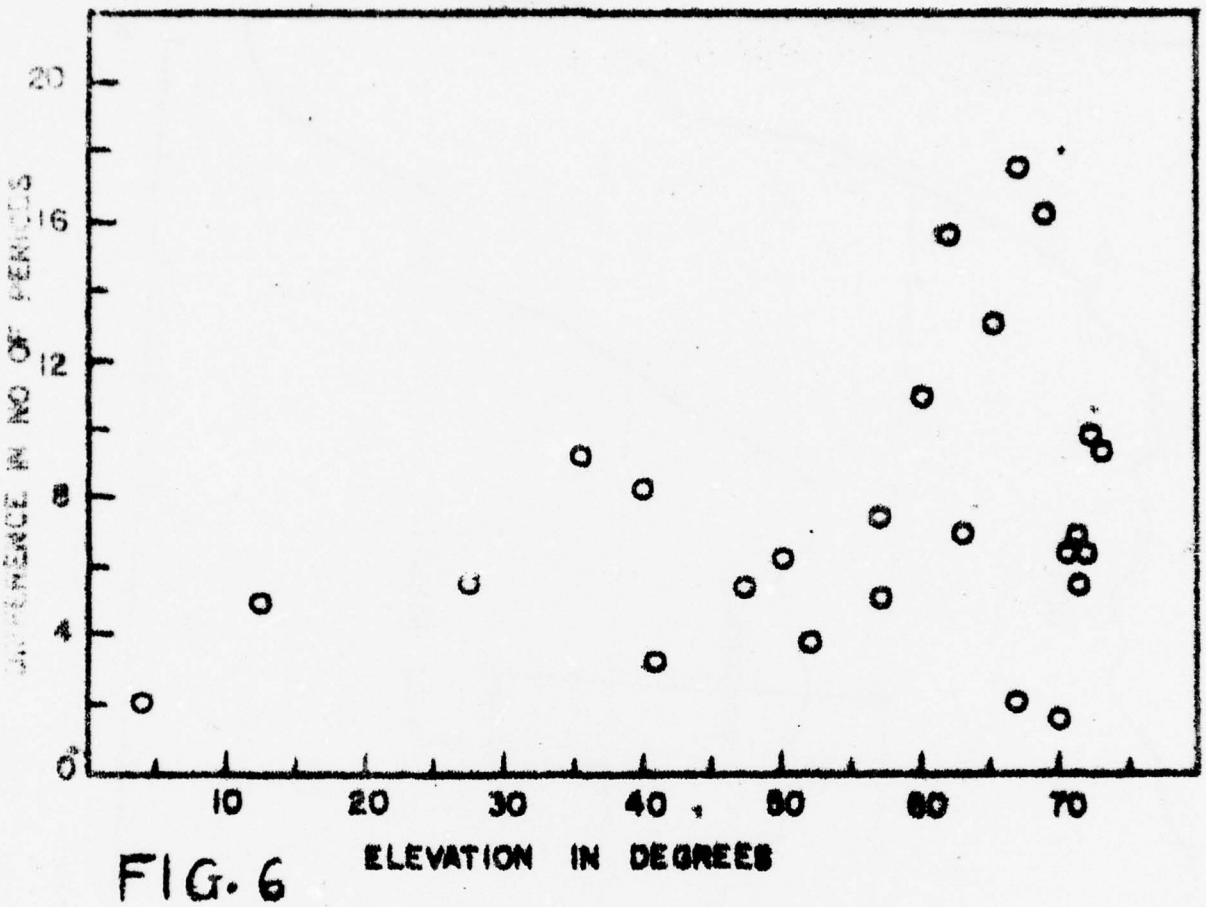

FIG. 6

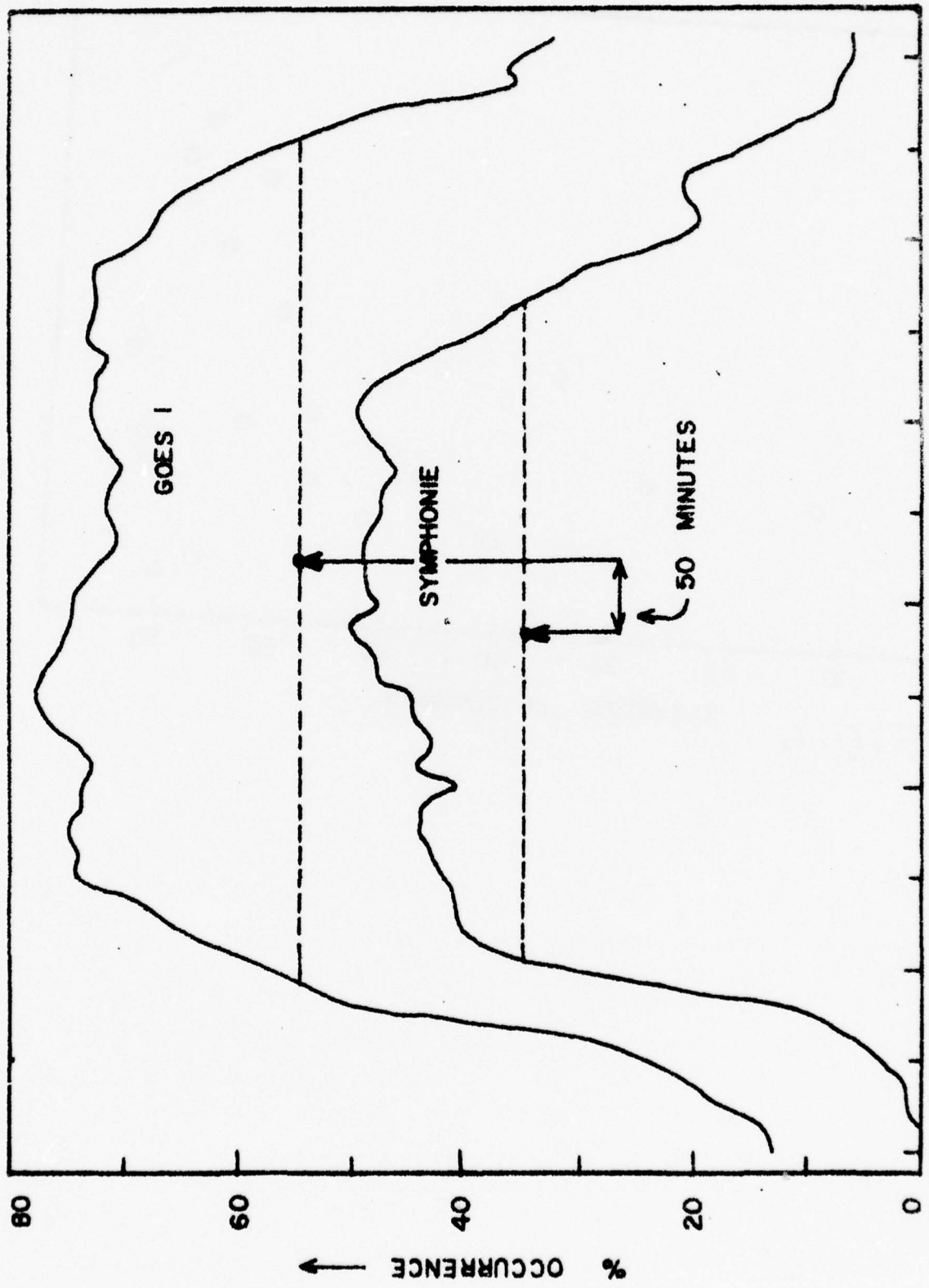
GOES I
SYMPHONIE
50 MINUTES
% OCCURRENCE
0
20
40
60
80
18
20
22
0
2
4
6
HOURS LOCAL TIME (GMT)

FIG. 7

CHAPTER 2

THE PHASE SWITCHING SYSTEM USED FOR SATELLITE SIGNAL AMPLITUDE MEASUREMENTS

1. INTRODUCTION

When faced with the problem of amplifying and measuring small d.c. or slowly changing a.c. signals, it is frequently advantageous to use a chopper to convert the signal to a.c., then to amplify this in a normal a.c. amplifier. A detector at the output can convert the result back to d.c. or slowly varying a.c. In this way the usually troublesome problems of d.c. amplifier drift are effectively circumvented.

In the simplest case, where a d.c. signal is turned into a.c. by a regular interruption of the connection to the amplifier input, the rectifier at the output of the a.c. amplifier will produce the same polarity, regardless of whether the input was derived from a positive or a negative d.c. source. This may be acceptable in some applications. In others, the signal polarity must be preserved at the amplifier output. This can easily be achieved by using a second output chopper, synchronized with the input chopper. A suitable filter to remove the chopping frequency will produce a d.c. or slowly varying a.c. signal, the polarity of which is dependent on the instantaneous polarity of the input signal. Such a detector, with an output chopper, is usually referred to as a "synchronous detector" or "phase sensitive detector". A widely used variation of this principle is found in the phase sensitive detectors used in interferometers in radio astronomy. Here the outputs from two separate aerials are combined alternately in phase and in antiphase at a convenient chopping frequency and amplified by a conventional receiver at any suitable intermediate frequency. The output from conventional detector and its following audio amplifier is then fed into a phase sensitive detector. Noise generated in either aerial alone, or in the receiver, itself effectively cancels, and even a very small signal can be recovered in the presence of noise many times larger than the signal itself.

The effectiveness of the phase sensitive detector in recovering a signal seemingly buried in noise lies in the fact that the effective bandwidth of the system can be made exceedingly narrow. If the phase sensitive detector is followed by a simple low pass RC filter, the effective bandwidth of the system is $2/T$ radians sec^{-1}, where $T = RC$, the time constant of the filter. Hence, the bandwidth is $2/(2\pi RC) = 1/(\pi RC)$ Hertz. A suitable choice of RC can make the effective bandwidth a small fraction of one Hertz - a bandwidth unattainable by any conventional filter circuit.

The interferometer described above can easily be adapted for use in measuring the total power received on a single aerial. The signal is split into two equal and 'in phase' components by a hybrid junction. These two signals are fed into the two inputs normally fed by the aerials of the interferometer. They are alternately combined in phase and in antiphase by the phase switch. The output of such a signal is directly proportional to the total power intercepted by the aerial times the cosine of the phase angle between them. Receiver noise cancels, but noise generated in the aerial contributes to the magnitude of the output.

2. THE OSCILLATOR

Figure 2.1(a) shows the oscillator used in the system. It is a conventional Wien bridge used in conjunction with a 741 operational amplifier. The circuit uses an n-channel junction gate field effect transistor as a variable resistor in the bridge circuit to stablize the oscillator amplitude. The frequency used in Legon is 800 Hertz, since this is the centre frequency of an audio filter built into the audio circuit of the Collins R 390 receiver normally used with the system. It is desirable, but not necessary to use this audio filter when operating the system. It filters out frequency components far removed from the chopping frequency, and helps prevent overloading of the phase sensitive detector. From this oscillator we derive both the a.c. signal needed to drive the diode switching unit (the chopper) and the reference signal needed for the phase sensitive detector. Provision must be made to shift the phase of the latter,

since it will have to be adjusted to compensate for any phase shift the signal may suffer in the receiver or in the detector.

3. THE DIODE SWITCHING UNIT

The diode switching unit, shown in Figure 2.1(b), consists of a 741 operational amplifier connected as a discriminator. Fed by the 800 Hertz sinusoidal voltage, it produces a square wave output. This output drives two GEX66 germanium diodes, connected in such a way that one conducts during the positive excursion of the square wave, the other during the negative excursion. These diodes terminate two quarter wavelength coaxial stubs that control the chopping of the signal, as described in the next paragraph.

4. THE PHASE SWITCH

Two versions of phase switches, either of which can be driven by the diode switching unit, are shown in Figure 2.2. The upper figure (A) is that of the conventional phase switch used in radio astronomy. All the lines shown are coaxial cable, and the circles represent coaxial junction boxes. When one of the diodes is conducting, the quarter wave stub to which it is attached is short circuited. This appears as an open circuit at the junction a quarter wavelength away, and hence a signal can pass from aerial 1 to the receiver through the junction in question. Meanwhile, the other diode is reverse biased, the corresponding stub is open circuited. This appears as a short circuit at the junction box, effectively preventing any signal from passing via the latter junction box to the receiver. When the diodes reverse, the signal takes the alternate path. Since one path is one wavelength long, the other one half wavelength, the signal arriving at the receiver junction is alternately in phase and in antiphase with that received from aerial 2 via a half wavelength path. The shorted quarter wave stub at the receiver junction is to provide a return d.c. path for the current driving the diodes.

A simpler version of a switch is shown in Figure 2.2(B). Operation is similar in principle, but here the receiver is alternately connected to the aerial and to a matched load. This version functions,

therefore, as a true chopper, and not as a phase switch.

5. THE PHASE SHIFTING AND SQUARING CIRCUIT

Figure 2.3 shows the circuit designed to provide a reference square wave for the phase sensitive detector. The first part of the circuit is a 741 operational amplifier designed to provide unity gain and an adjustable phase shift through 180° relative to the oscillator. This feeds a second 741 connected as conventional discriminator. The non-inverting input of the 741 goes to a variable d.c. voltage, adjustment of which provides control of the mark-space ratio at the output of the discriminator. This circuit, together with that for the phase sensitive detector, is taken from Clayton (1975).

6. THE PHASE SENSITIVE DETECTOR

The circuit shown in Figure 2.4(a) is the relatively simple phase sensitive detector used in the more recent Legon equipment. This circuit is taken from Clayton (1975), and since it is fully described there, we shall say little about it. The values of R and C at the output can be chosen to meet the requirements of the particular application. The values shown in the drawing (100k ohms and 69 microfarads) yield an output time constant of 6.9 seconds. The value actually used for our MARISAT 1 experiments was 100k and 2.2 microfarads, yielding a time constant of 0.22 seconds, and a bandwidth of 1.4 Hertz.

The operation of phase sensitive detectors is easiest to express quantitatively if we look at them from the point of view of voltage multipliers, which they are. Two voltages, V_s and V_r are multiplied in the circuit, and the output voltage V_o is their product. Four separate cases present themselves.

(a) If identical input signals are presented at the two inputs,

we have: $V_o = V_i^2 \cos^2\omega t = V_i^2(1 + \cos(2\omega t))/2$

Hence, here the circuit gives a d.c. component (rectification) and a component at twice the input frequency (frequency doubling).

(b) If V_s and V_r have the same frequency, but different phases, we get: $V_o = V_s V_r \cos(\omega t)\cos(\omega t + \phi)$

$$= (V_s V_r/2) \times (\cos(2\omega t + \phi) + \cos(\phi))$$

Here we have a case of frequency doubling, with a d.c. component proportional to the cosine of the phase difference. This is a phase sensitive detector. The reference is normally adjusted to $\phi = 0$, so that the d.c. component is a maximum. The a.c. component is filtered out.

(c) If two different inputs are used - differing, that is, in amplitude and frequency, one gets the following:

$$V_o = V_s V_r \cos(\omega_1 t) \cos(\omega_2 t)$$

$$= (V_s V_r/2) \times (\cos(\omega_1 + \omega_2)t + \cos(\omega_1 - \omega_2)t)$$

i.e., we get an output containing sum and difference frequencies.

(d) If one frequency is zero - i.e., a d.c. signal is applied, the output voltage is given by

$$V_o = V_r V_s \cos(\omega t)$$

i.e., the multiplier acts as a voltage controlled attenuator.

If, as is usually the case, we use a large square wave as reference, a mathematical analysis requires that we express this as a Fourier series, and consider the Fourier components separately. This is done by Clayton (1975).

Results show that there should be d.c. components from the various harmonics, but they are much smaller than that from the fundamental frequency. The assumption here is that the bandwidth in the radio and audio frequency sections of the receiver is wide enough to pass the harmonics of the chopping frequency, as well as the fundamental. It is also assumed that the phase shift is constant for the harmonics. In practice, these assumptions do not seem to be realized, and experiments at Legon have shown that there is little or nothing to be gained by

using a wide audio bandwidth and trying to get the additional d.c. contributions of the harmonics. Hence, it is recommended that the audio filter in the R 390 be used, effectively limiting the result to the fundamental of the chopping frequency.

7. THE D.C. AMPLIFIER

The circuit in Figure 2.4(b) is an optional addition to the circuit that may be found useful in driving a pen recorder if the output of the phase sensitive detector itself is too small for this purpose. In addition, it provides an adjustable 50 Hertz component superimposed on the d.c. output. This can be used as an anti-stick device, to decrease the response time of pen recorders where friction between pen and paper would otherwise cause an extremely slow response to small deflections.

REFERENCES

CLAYTON, G.B., 1975 Experiments With Operational Amplifiers; MacMillan Press Ltd., London.

TITLES OF FIGURES FOR CHAPTER 2

FIGURE 2.1 (a) The Wieh Bridge oscillator.

FIGURE 2.1 (b) The diode switching unit.

FIGURE 2.2 A true phase switch (A) and a chopper (B).

FIGURE 2.3 Phase shifting and squaring circuit to provide a reference square wave.

FIGURE 2.4 (a) The phase sensitive detector.

FIGURE 2.4 (b) An optional d.c. amplifier with provision for anti-stick.

OSCILLATOR (WIEN BRIDGE)

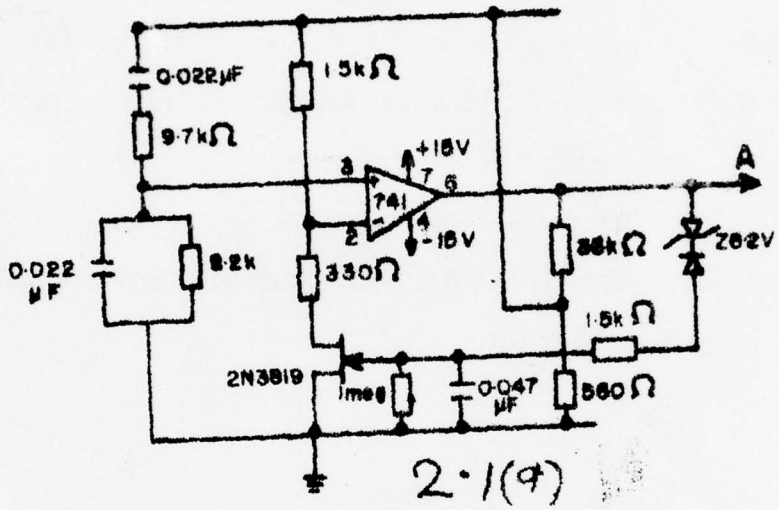

2·1(a)

DIODE SWITCHING UNIT

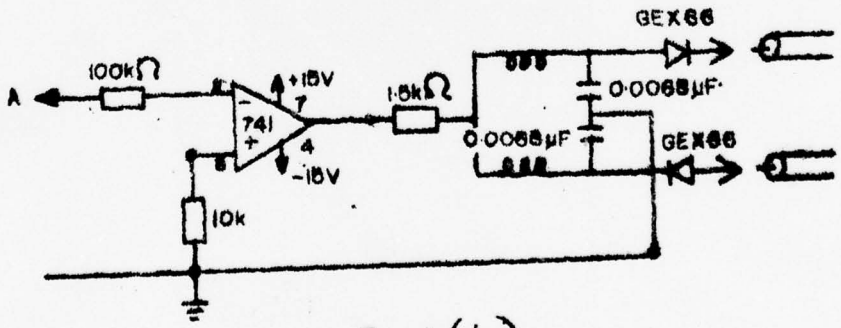

2·1(b)

(A)

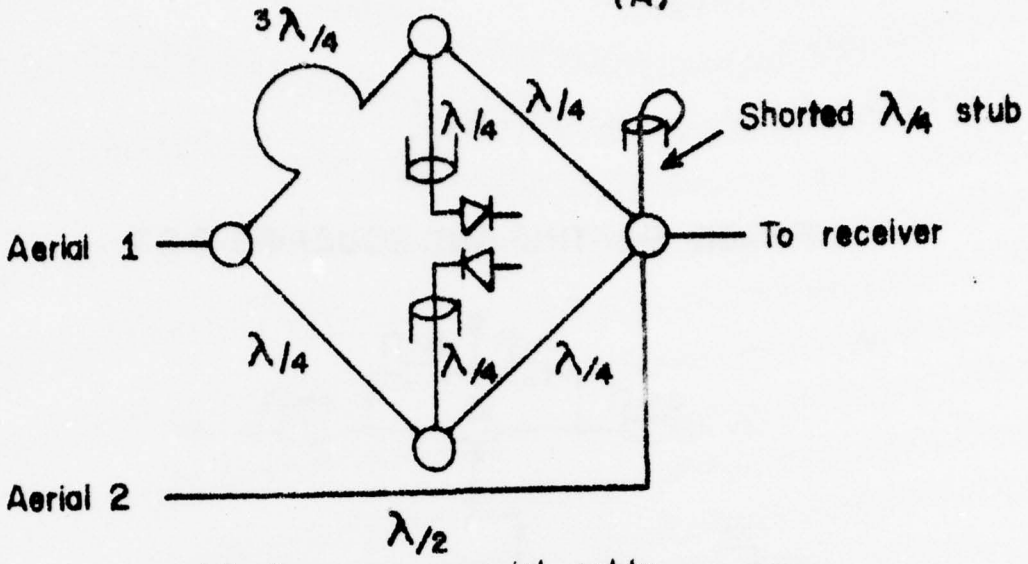

All lines are coaxial cable

(B)

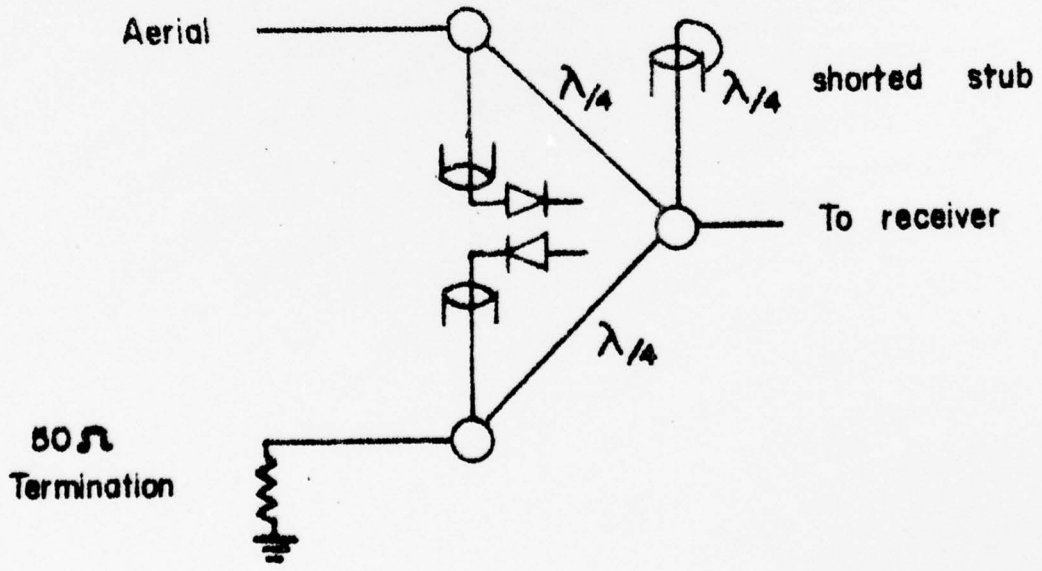

All lines are coaxial cable

2·2

PHASE SHIFTING AND SQUARING C C T.

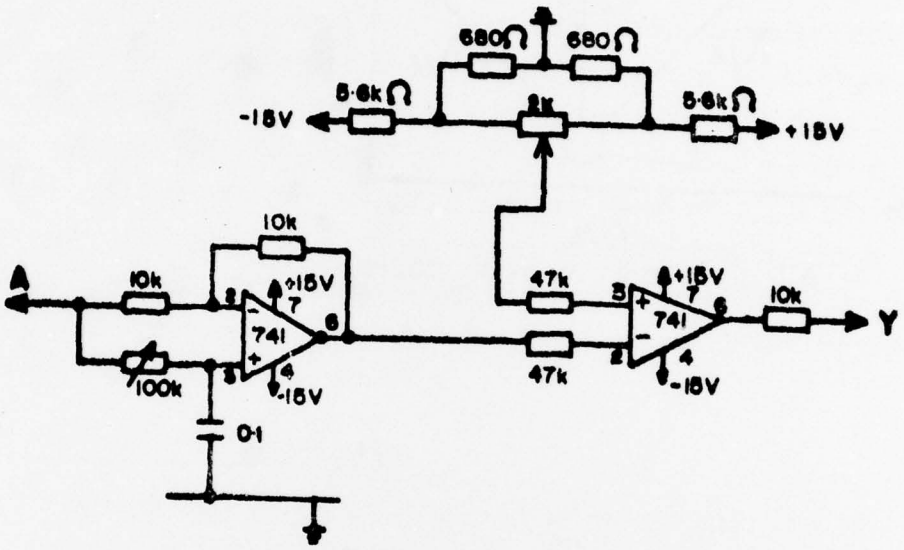

2·3

PHASE SENSITIVE DET.

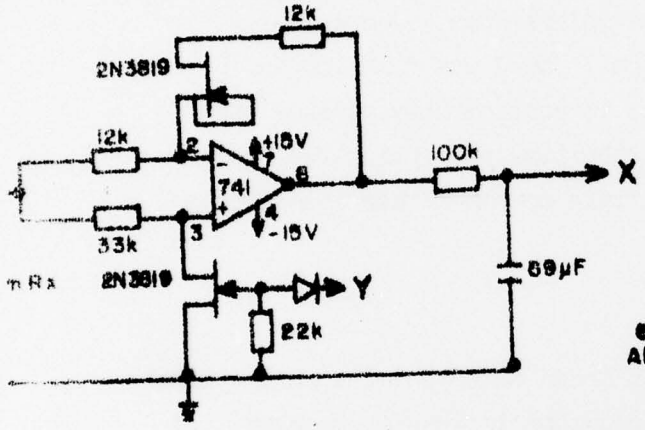

2·4(a)

DC. AMP.

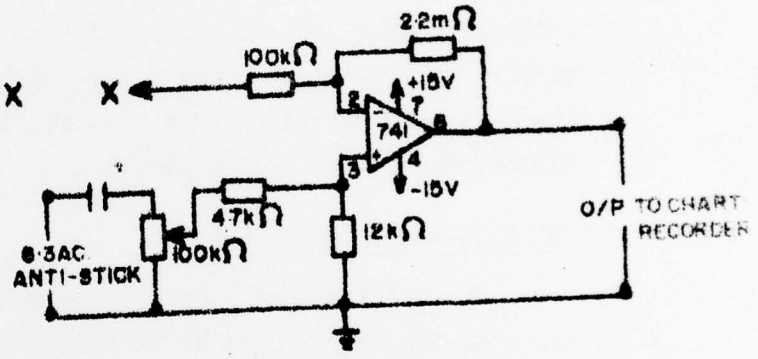

2·4(b)

CHAPTER 3

THE LEGON POLARIMETER

1. INTRODUCTION

The polarimeter used at Legon for the determination of the Faraday rotation imposed by the ionosphere on plane polarized waves emitted by synchronous satellites has been described before, but we give a brief description of it here, and go on to describe for the first time an analogue output device which has been used for the past three or four years. The polarimeter, as originally designed, produces only a digital output. Need was felt for an analogue output as well, to enable one to continuously monitor the output, as well as to provide much higher time resolution for those relative rare occasions when a solar flare or some other ionospheric disturbance render this desirable.

2. THE ORIGINAL POLARIMETER

The original polarimeter used at Legon made use of a phase switching interferometer, similar to that described in Chapter 2 above. It will be recalled that the instrument has two inputs. Signals derived from two oppositely wound helical aerials of indentical gain are fed into the inputs. These are periodically (at a frequency of 800 Hertz) connected in phase and in antiphase. When signals of the same frequency, but differing phase, are fed into such an instrument, the output is proportional to $V_1V_2 \cos \emptyset$, where V_1 and V_2 are the two input voltages, and $\emptyset$ is the phase angle between them. In such an instrument, noise generated in the receiver, as well as noise picked up by only one of the two aerials is effectively cancelled in the phase sensitive detector. An extremely narrow effective bandwidth can be achieved by using a large time constant in the output of the phase sensitive detector.

It might be mentioned here that it is sometimes desirable to derive right and left hand circularly polarized signals from the same aerial, by using crossed Yagis in conjunction with a magic tee. This

is often an advantage when the satellite is not stationary, and when its motion would produce an additional phase change in aerials physically separated from one another.

One could derive the phase angle directly from the amplitude of the output voltage. But V_1 and V_2 are often slowly varying with time, and it is troublesome to continuously monitor their separate amplitudes. Consequently, the polarimeter was designed to make use of a slow ring counter (1 second per step) to drive 6 transistor drivers. (See Figure 3.1). Each of these drivers control three reed switches, connected in parallel. Two of these reed switches connect an extra length of coaxial cable into the aerial lead from one of the helices. The third switch in each set connects the output of the phase sensitive detector to one of six series RC pairs. The values of R and C in these 6 series pairs are identical, and are chosen so that the time constant is long enough to smooth fluctuations occuring during times of severe scintillation. Time constants of the order of 1 to 10 seconds are used. The relatively slow switching speed of 1 per second is used to prolong the service life of the reed switches.

At any given instant, each of the 6 capacitors in the output RC pairs is at a voltage $V_1V_2 \cos(\emptyset + \alpha)$, where α is the electrical length of the extra cable switched into the aerial lead. Since these were selected to be 60°, 120°, 180°, 240°, 300° and 360° in electrical length, the six voltages present at the output lie along a cosine curve, at 6 equally spaced points. From these voltages, sampled every 10 minutes and printed out by a data logger, it is possible to determine $\emptyset$ uniquely. The determination is actually done by a least squares curve fitting program on a digital computer.

3. THE ANALOGUE OUTPUT

In addition to the digital output, an analogue output, presented on a strip chart recorder, was highly desirable. A separate circuit was designed to provide this. It is made up of the following elements:

(a) A fast ring counter, driven by a 6 KHz square wave oscillator. This counter is a standard one, and its circuit is shown in Figure 3.2.

(b) Six control voltages, one derived from each stage of the ring, control two sets of 6 integrated circuit analog switches. These are normally off, but turned on in sequence by the control voltages.

(c) The input to each switch of one set of six is connected to one of the 6 capacitors in the output of the phase sensitive detector described earlier. (See Figure 3.3).

(d) The six switch outputs are connected together, giving a set of six "steps" approximating the cosine function described in the previous paragraph.

(e) This step function is smoothed by means of a parallel tuned LC circuit resonant at 1 KHz.

(f) The second set of six analog switches have three inputs connected to a d.c. source; three connected to earth. The outputs are paralleled, and produce a reference square wave. The power supply for the circuit at Fig.3.3 is given in Figure 3.4.

(g) The 1 KHz cosine wave and the reference square wave are fed into a conventional phase meter, and the output of the phase meter is recorded on a strip chart recorder. The diagram for the locally constructed phase meter appears in Figure 3.5(a) and (b). Its power supply is given in Figure 3.6.

TITLES OF FIGURES FOR CHAPTER 3

FIGURE 3.1. Slow ring counter to drive 6 sets of 3 reed switches. Two of each set of switches insert an additional length of coaxial cable into one aerial lead. The third controls the output from the phase sensitive detector.

FIGURE 3.2. Fast ring counter for analogue output device.

FIGURE 3.3. Circuit to generate an analogue output. It generates a 1 KHz sine wave from the 6 outputs of the phase sensitive detector. It also produces a reference square wave.

FIGURE 3.4. Power supply for the circuit in Figure 3.3.

FIGURE 3.5(a) and (b) The phase meter used in the analogue output circuit.

FIGURE 3.6 Power supply for the phase meter.

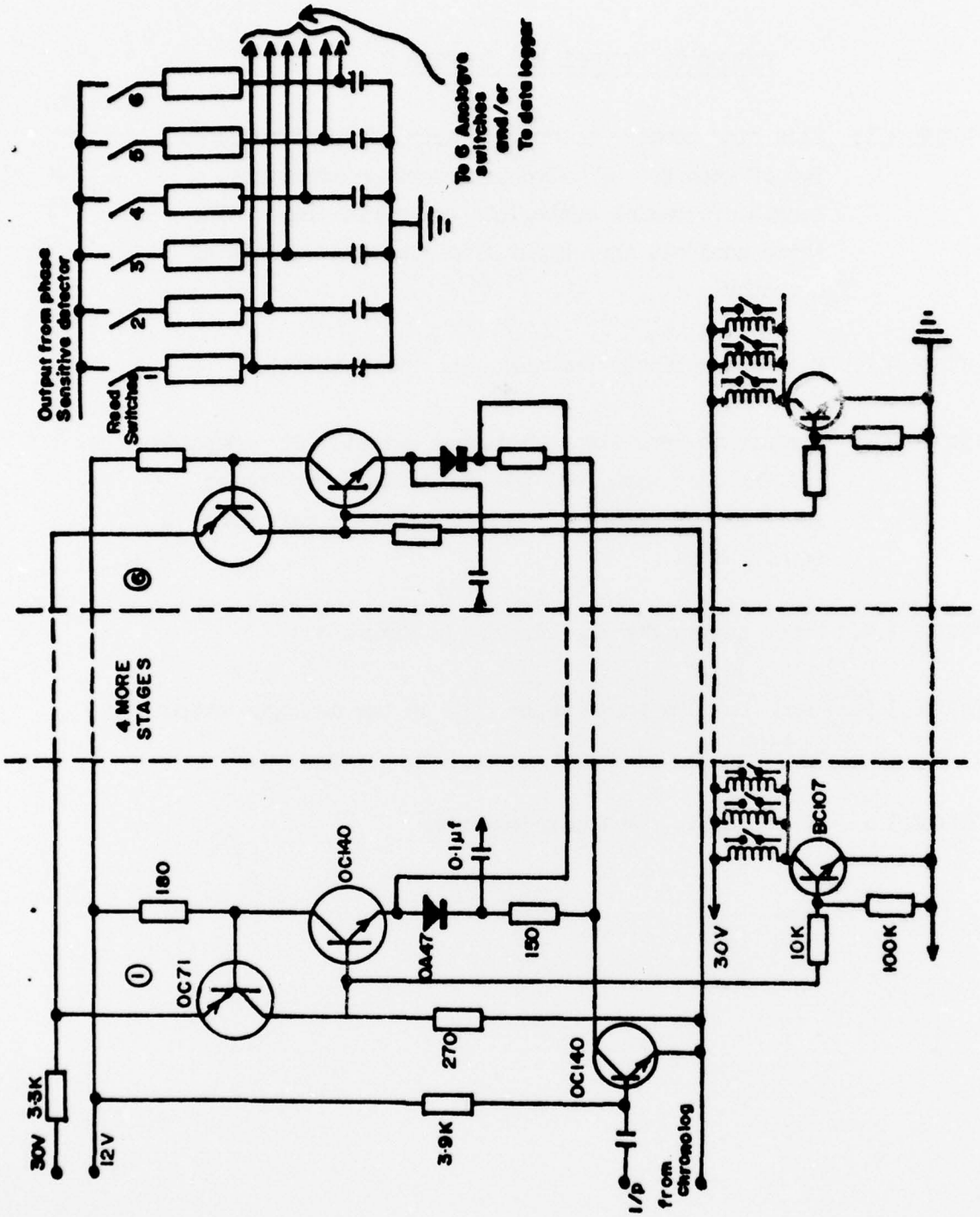
Output from phase Sensitive detector
Reed Switches
To 6 Analogue switches and/or To data logger
4 MORE STAGES
OC71
OC140
OC140
OA47
0·1µf
180
150
270
3·9K
33K
30V
12V
10K
100K
BC107
I/p from chronolog

3-1

RING COUNTER DIAGRAM

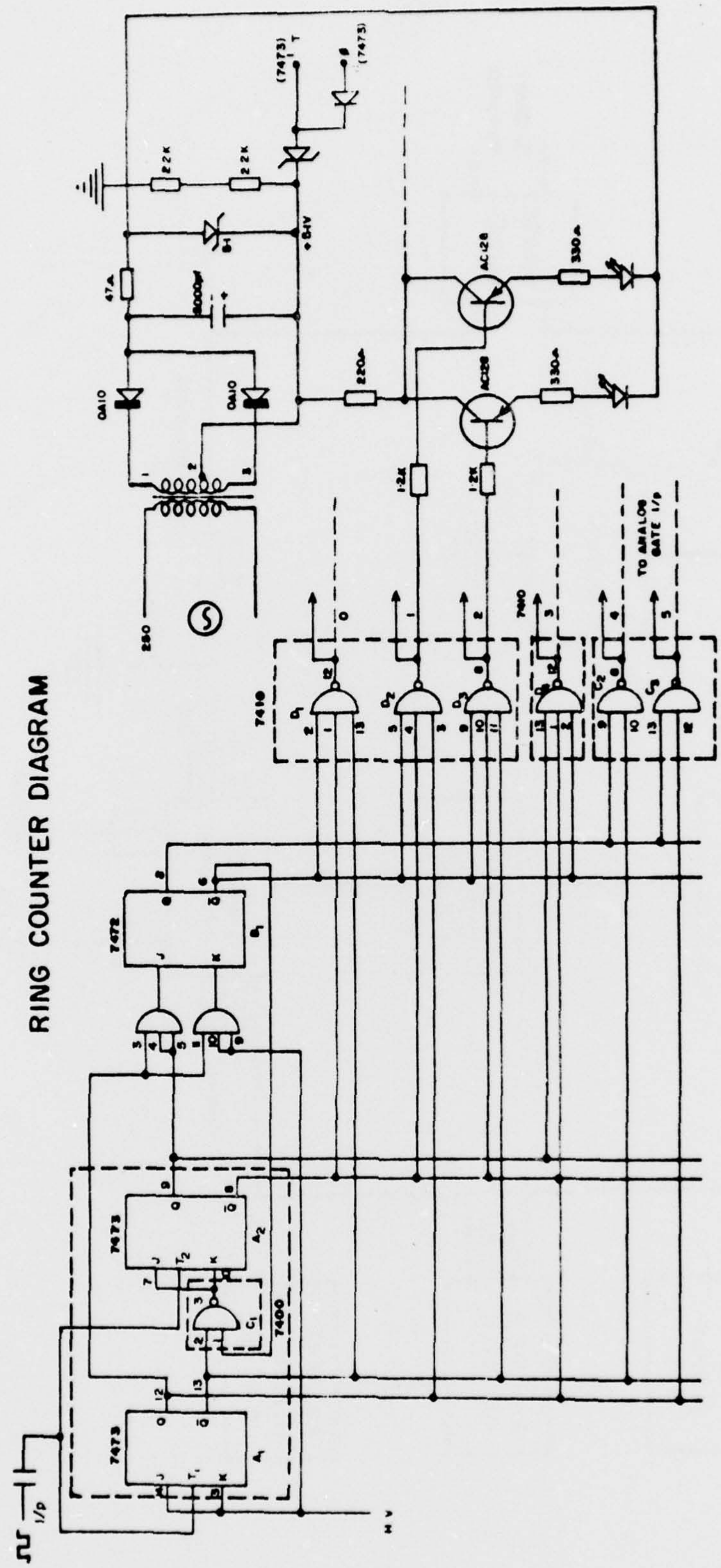

3.2

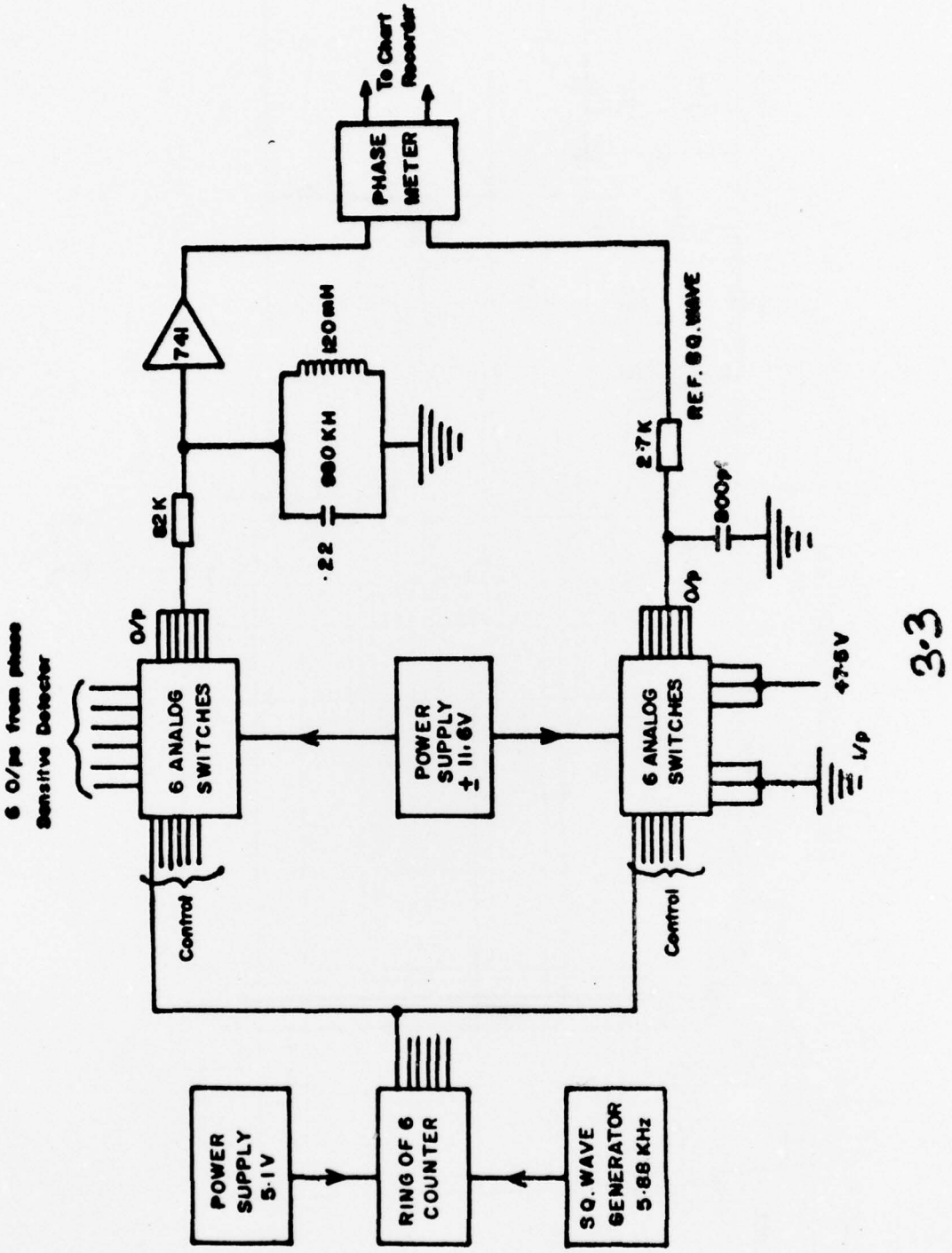
To Chart Recorder
PHASE METER
741
120mH
680 KH
.22
82K
2·7K
REF. SQ. WAVE
800pf
O/p
6 O/ps from phase Sensitive Detector
6 ANALOG SWITCHES
POWER SUPPLY ± 11·6V
6 ANALOG SWITCHES
Control
Control
47·6V
I/p
POWER SUPPLY 5·1V
RING OF 6 COUNTER
SQ. WAVE GENERATOR 5·88 KHz

3·3

± 11·6V POWER SUPPLY FOR DG201 ANALOG SWITCH

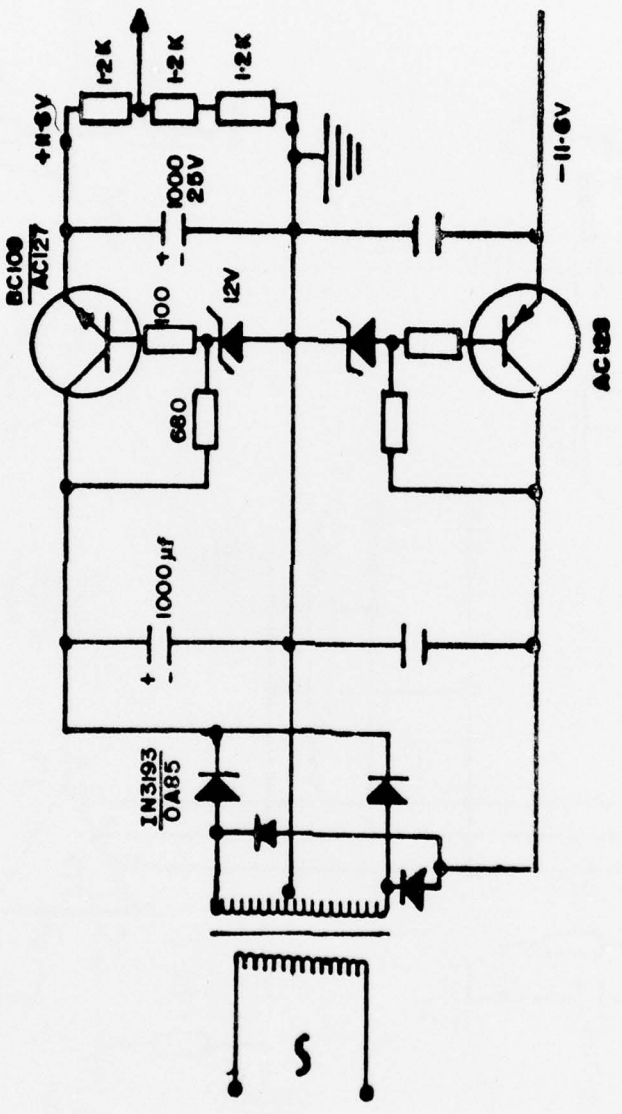

3·4

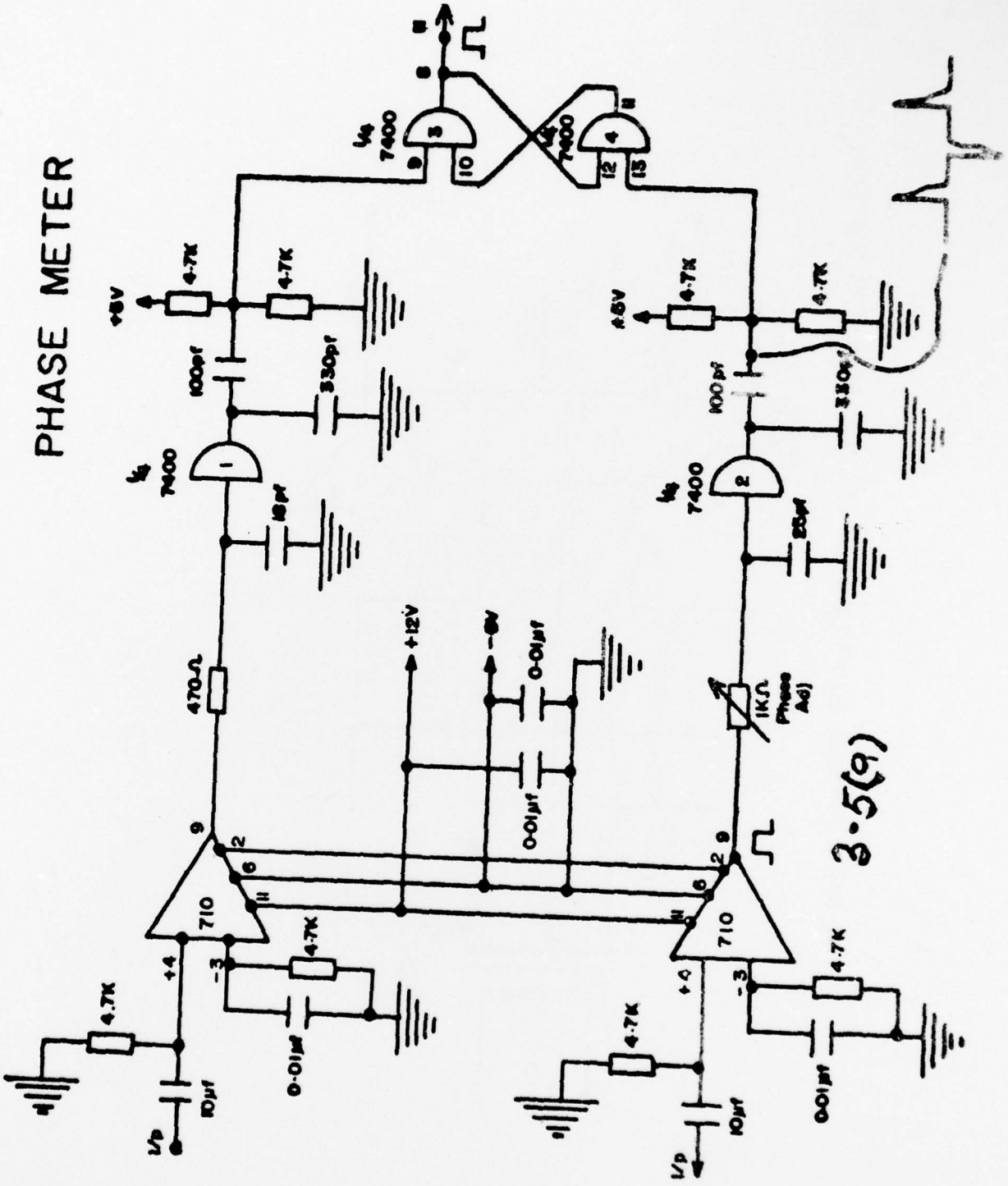
PHASE METER
7400
4.7K
100pf
330pf
18pf
20pf
470Ω
1KΩ Phase Adj
+12V
-6V
0·01μf
10μf
710
3·5(9)

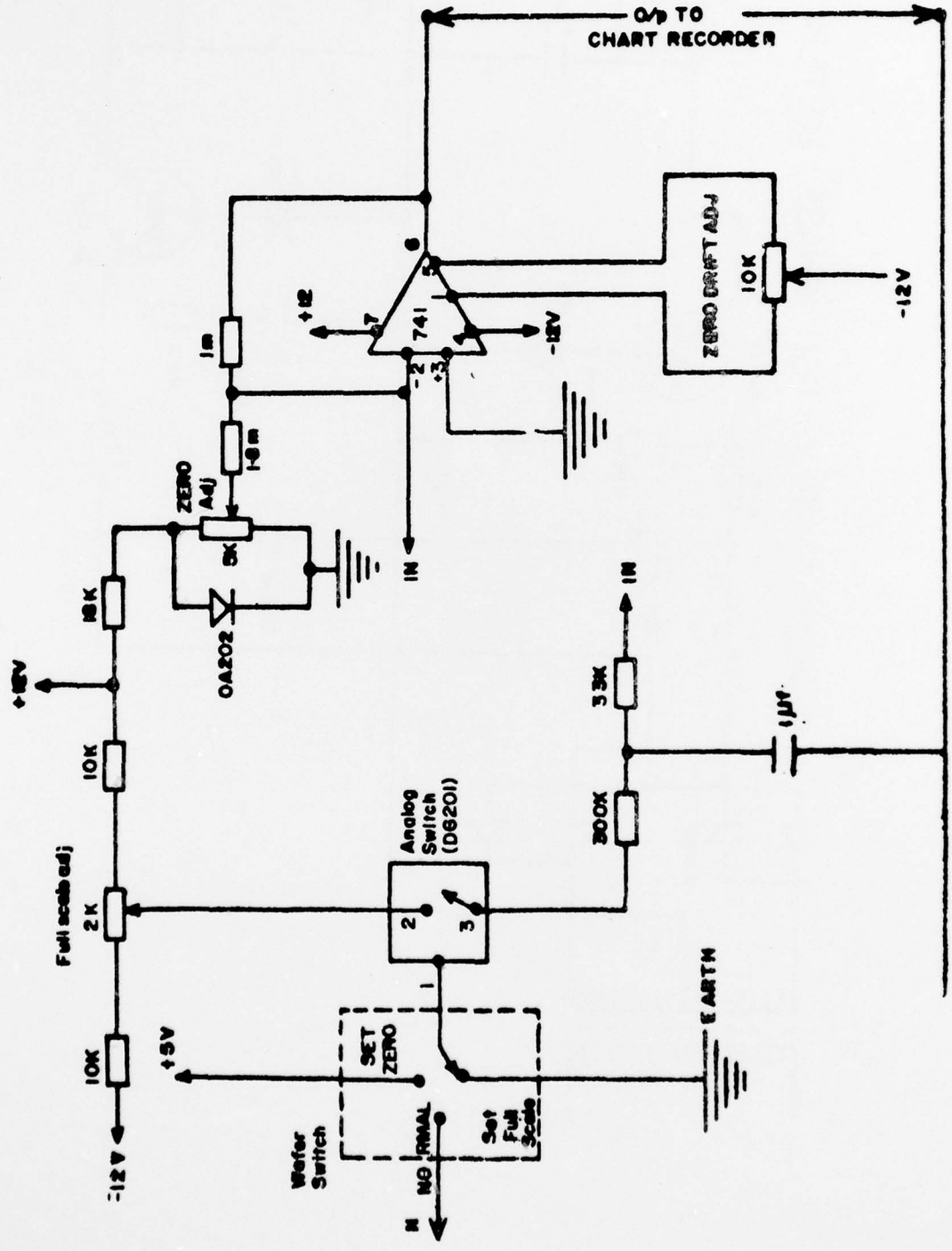
O/p TO
CHART RECORDER
ZERO DRIFT ADJ
10K
-12V
+12
741
-18V
1m
1·8m
ZERO
Adj
5K
OA202
IN
+18V
18K
10K
Full scale adj
2K
10K
-12V
+5V
SET
ZERO
Wafer
Switch
NORMAL
Set
Full
Scale
N
Analog
Switch
(DG201)
33K
IN
1μF
300K
EARTH

3·5(b).

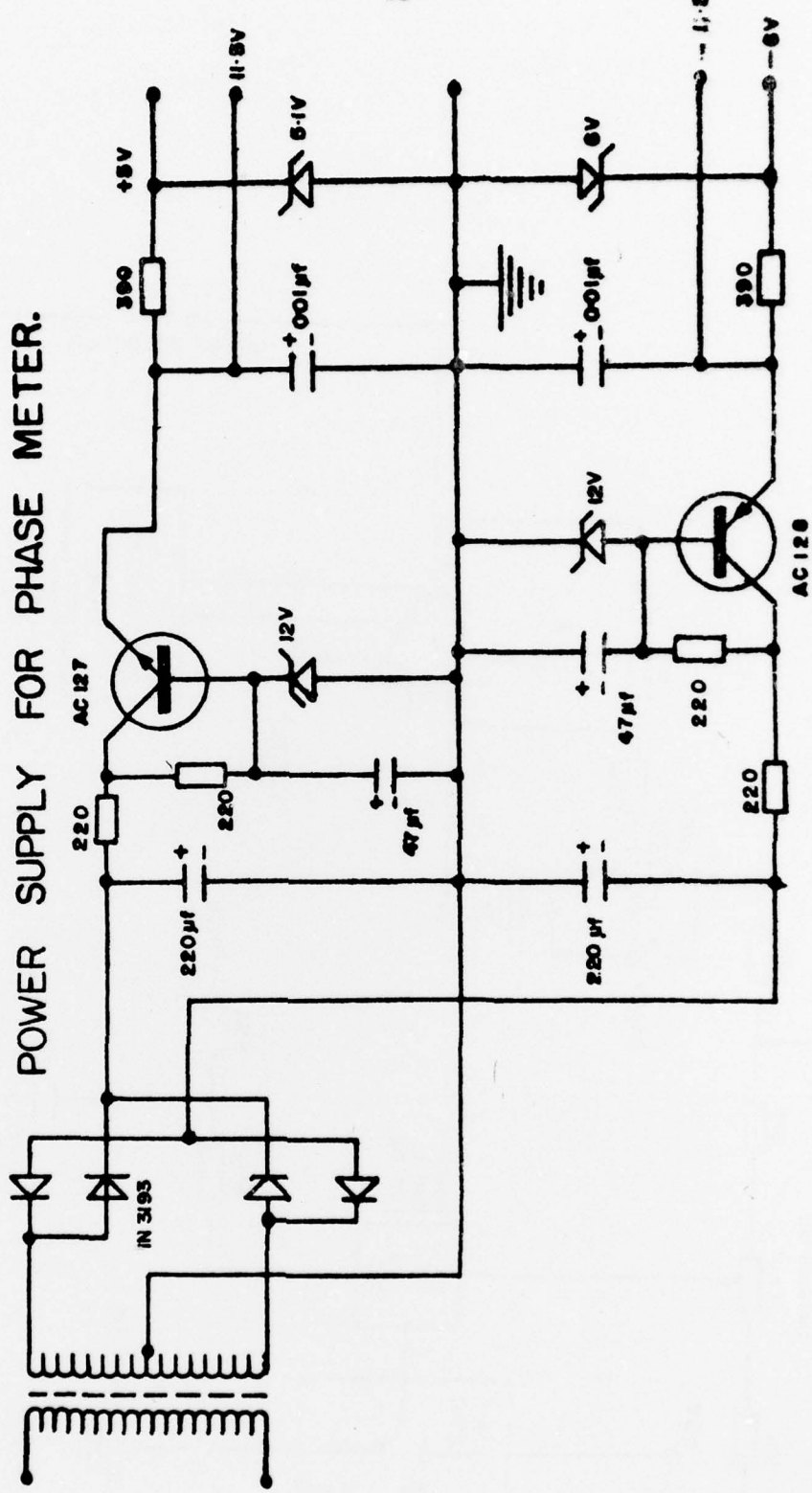
POWER SUPPLY FOR PHASE METER.
+5V
11·5V
6·1V
6V
-11·5V
-6V
390
390
·001µf
·001µf
12V
12V
AC127
AC128
220
220
47µf
47µf
220
220
220µf
220µf
IN 393

3·6

Printed by
United States Air Force
Hanscom AFB, Mass. 01731